E. DEMİR

DESIGN OF COOLED AND HEATED CABINET BY USING LIQUID NITROGEN

THE GRADUATE SCHOOL OF NATURAL AND APPLIED SCIENCES
OF
ATILIM UNIVERSITY

EMRE DEMİR

A MASTER OF SCIENCE THESIS
IN
THE DEPARTMENT OF MECHANICAL ENGINEERING

JANUARY 2024

ATILIM UNIVERSITY 2024

DESIGN OF COOLED AND HEATED CABINET BY USING LIQUID NITROGEN

A THESIS SUBMITTED TO
THE GRADUATE SCHOOL OF NATURAL AND APPLIED SCIENCES
OF
ATILIM UNIVERSITY

EMRE DEMİR

A MASTER OF SCIENCE THESIS
IN
THE DEPARTMENT OF MECHANICAL ENGINEERING

JANUARY 2024

Approval of the Graduate School of Natural and Applied Sciences, Atılım University.

_____

Prof. Dr. Ender KESKİNKILIÇ
Director

I certify that this thesis satisfies all the requirements as a thesis for the degree of **Master of Science in Mechanical Engineering at Atılım University**.

_____

Prof. Dr. Sadık Engin KILIÇ
Head of Department

This is to certify that we have read the thesis DESIGN OF HEATED AND COOLING CABINET BY USING LIQUID NITROGEN AND HEATERS submitted by EMRE DEMİR and that in our opinion it is fully adequate, in scope and quality, as a thesis for the degree of Master of Science.

_____

Assoc. Prof. Dr. Cihan TURHAN
Supervisor

Examining Committee Members:

Assoc. Prof. Dr. Cihan TURHAN _____
Energy Systems Engineering Department Atılım University

Asst. Prof. Dr. Bahram Lotfi SADIGH _____
Mechanical Engineering Department Atılım University

Asst. Prof. Dr. Ferit SAİT _____
Mechanical Engineering Department Çankaya University

Date: *19.01.2024*

I hereby declare that all information in this document has been obtained and presented in accordance with academic rules and ethical conduct. I also declare that, as required by these rules and conduct, I have fully cited and referenced all material and results that are not original to this work.

Name, Last Name: Emre, DEMİR

Signature:

ABSTRACT

DESIGN OF COOLED AND HEATED CABINET BY USING LIQUID NITROGEN

DEMİR, Emre

M.Sc, Department of Mechanical Engineering

Supervisor: Assoc. Prof. Dr. Cihan TURHAN

January 2024, 73 pages

In Türkiye, there is an increasing dependence on the importation of cryogenic conditioning chambers and associated specialized components within the defense industry, medical sector, and industrial domains. The indigenization of critical technologies, particularly in fields such as national defense, holds the promise of significant contributions to both national defense capabilities and economic growth. In this context, this thesis designs a specialized hot-cold air conditioning cabinet (chamber) which is capable of accommodating the requisite physical tests following temperature conditioning at prescribed levels. Specifically, the required operating temperatures for conditioning are set at -55°C and +70°C for cold and enviroments, espectively. The primary application of this chamber is directed towards the rigorous testing and validation of aviation and space equipment. While chambers of this nature have been previously designed for scientific and medical use. The distinctive feature of this study is its flexible design, enabling usage for large volumes. This flexible design not only broadens application areas but also enhances user-friendliness of construction. Moreover, the chamber can be separated into two components for loading or unloading testing equipment and can be easily transported

using wheel or lifting equipment design. This allows conditioned equipment to undergo lifetime tests at the desired conditioning temperatures.

In this thesis, the required coolant capacity for cooling the useful load was calculated, heat flux from the walls, and insulation thicknesses were determined, respectively and accordingly. From the beginning of the design to the manufacturing process, all thermal bridges, heat leakagess, and heat transfer points were examined during the design phase, and thermal performance was improved through various material uses and design changes. Moreover, the structural geometries of the cabinets were scrutinized and analyzed. Static analyses were conducted using Ansys Mechanical, considering working conditions to prevent potential deformations in the cabinets. Mesh metric values from these analyses were examined, and geometric corrections were made accordingly based on the output of these analyses. The direct application of cryogenic liquids, thanks to their rapid cooling performance, can expand the scope of use in aviation and space equipment tests. Similar studies can be applicable to other cryogenic liquids or diversified through geometric revisions to extend their application areas.

Keywords: Cryogenic Cooling, Aviation and Space, Ansys Workbench Mechanical

ÖZ

SIVI AZOT KULLANARAK ISITMA VE SOĞUTMA KABİNİ TASARIMI

DEMİR, Emre
Yüksek Lisans, Makine Mühendisliği Bölümü
Danışman: Doç. Dr. Cihan TURHAN

Ocak 2024, 73 sayfa

Ülkemizde, savunma endüstrisi, tıbbi sektör ve endüstri alanlarında kriyojenik koşullandırma dolapları ve ilişkili özel bileşenlerin ithaline yönelik artan bir bağımlılık bulunmaktadır. Özellikle ulusal savunma gibi kritik teknolojilerin yerlileştirilmesi, hem ulusal savunma kabiliyetlerine hem de ekonomik büyümeye önemli katkılar vaat etmektedir. Bu bağlamda, bu tezde, belirlenmiş seviyeler için sıcaklık koşullandırmasını takiben gerekli fiziksel testlere uygun olan özel bir sıcak-soğuk koşullandırma kabini tasarlanmış ve analiz edilmiştir. Özellikle, koşullandırma için hedef işletme sıcaklıkları -55°C ve 70°C olarak belirlenmiştir. Bu kabinin başlıca uygulaması, havacılık ve uzay ekipmanlarının titiz test ve doğrulaması içindir. Bu tür dolaplar daha önce bilimsel ve tıbbi kullanım için tasarlanmıştır. Bu çalışma ile diğerlerinin arasındaki fark, tasarımının esnek olması ve büyük hacimler için kullanılabilecek olmasıdır ve kullanım alanlarını genişletirken aynı zamanda kullanım kolaylığı sağlar. Öte yandan, dolap, test ekipmanını yüklemek veya boşaltmak için iki bileşene ayrılabilir ve tekerlek veya kaldırma ekipmanı ile kolayca taşınabilir. Bu sayede şartlandırılmış ekipmanlar ile ömür testleri istenilen şartlandırma koşullarında gerçekleştirebilir. Tez çalışması için faydalı yükü soğutmak amacıyla gerekli soğutucu akışkan miktarı hesaplanmıştır. Duvarlardan gelen ısı akısı hesaplanmış ve buna göre yalıtım kalınlıkları tayin edilmiştir. Tasarımın başlangıcından imalat sürecine kadar, tasarım aşamasında tüm termal

köprüler, ısı sızıntıları ve transfer noktalarını incelenmiş ve çeşitli malzeme kullanımları ve tasarım değişimleri ile termal performans iyileştirilmiştir.

Kabinlerin yapısal geometrileri incelenmiş ve analiz edilmiştir. Kabinlerde oluşabilecek deformasyonların önüne geçebilmek için Ansys Mechanical programı üzerinden çalışma koşulları göz önüne alınarak statik analizler yapılmıştır. Bu analizlere ait mesh metrik değerleri incelenmiş ve bu analiz çıktılarına uygun olarak geometrik düzeltmeler yapılmıştır. Doğrudan kriyojenik sıvı uygulamalarının, hızlı soğutma performansı sayesinde, havacılık ve uzay ekipmanı testlerinde kullanım alanı genişletilebilir. Benzer çalışmalar başka kriyojenik sıvılar için uygulanabilir ya da geometrik revizeler ile kullanım alanları çeşitlendirilebilir.

Anahtar Kelimeler: Kriyojenik Soğutma, Havacılık ve Uzay, Ansys Workbench Mechanical

To my family…

ACKNOWLEDGMENTS

I sincerely thank my advisor, Assoc. Prof. Dr. Cihan Turhan, for guiding me and generously providing support throughout this research process. Additionally, I express my gratitude to the Promec Engineering Ltd R&D Team for their contributions to the successful completion of the project.

I owe a special thanks to my family, who have been by my side, and to my dear spouse, who continuously supported and encouraged me, playing a significant role in achieving this success. Without their support, reaching this milestone would not have been possible. I sincerely thank each of you for the support and trust you have given.

TABLE OF CONTENT

LIST OF TABLES

TABLES

LIST OF FIGURES

FIGURES

LIST OF SYMBOLS

c	Specific Heat (J/g°C)
T	Temperature (°C)
λ	Latent Heat of Vaporization (J/g)
c_{pf}	Isobaric Spesific Heat of Vapor (J/g°C)
θ	Heat Transfer (Watts)
m	Mass (Kg)
ɞ	Spesific Liquid Requirment
R	Ideal Gas Constant (J/(mol K))
V	Volume (m^3)
e_1	Lenght (mm)
W	Watt
A	Surface Area (m^2)
R_{to}	Thermal Resistance Per Unit Area (K·m²/W)
∅	Heat Energy (Joules)
λ	Thermal Conductivity
h	Specific Enthalpy(J/Kg)
ΔT	Temperature Change (°C)
SUBSCRIPTS	
a	Initial Value
c	Final Value
e	Equipments
f	Fluids
min/max	Min/max Value of Variable
g	Gas
to	Total Value

CHAPTER 1

CRYOGENICS COOLING

Cryogenics, as a scientific discipline, focuses on the production and consequences of extremely low temperatures. The term "cryogenics" finds its roots in the Greek words "kryos," which translates to "cold," and "genic," meaning "generation" or "production." While this definition could theoretically encompass all temperatures below the freezing point of water (0°C), it was Professor Kamerlingh Onnes of Leiden University in the Netherlands who, in 1894, first coined the term to describe the science and art of achieving significantly lower temperatures. He specifically employed the term in the context of liquefying permanent gases such as oxygen, nitrogen, hydrogen, and helium. Notably, oxygen had been liquefied at -183°C a few years earlier in 1887, sparking a race to further liquefy the remaining permanent gases at even lower temperatures. The techniques employed to reach these extremely low temperatures differed significantly from those used in the earlier production of artificial ice and necessitated efficient heat exchangers.

As per the principles of thermodynamics, there exists an unattainable limit for the lowest achievable temperature, known as " absolute zero". At the absolute zero, molecules are in their lowest but still finite energy state. Achieving this temperature is practically impossible because the required energy input approaches infinity. Nevertheless, scientists have managed to reach temperatures within a few billionths of a degree above absolute zero. Absolute zero is precisely defined as -273.15°C or -459.67°F. The internationally accepted metric system, the Kelvin scale, uses the symbol K and has the same magnitude as the degree Celsius. The Kelvin scale was adopted in 1968 by the 13th General Council on Weights and Measures (CGPM). In the Kelvin scale, 0°C corresponds to 273.15 K. In contrast, the English absolute scale, known as the Rankine scale, uses the symbol R and has increments equivalent

to those of the Fahrenheit scale. In terms of the Kelvin scale, the cryogenic region is often regarded as temperatures below approximately 120 K (-153°C) [1].

1.1 The Historical Development of Cryogenic Science

The historical development of cryogenic science is marked by significant milestones and breakthroughs that have paved the way for modern applications and scientific exploration. It all began in the 17th century with the determination of the freezing point of seawater, a fundamental step that laid the foundations for cryogenic science.

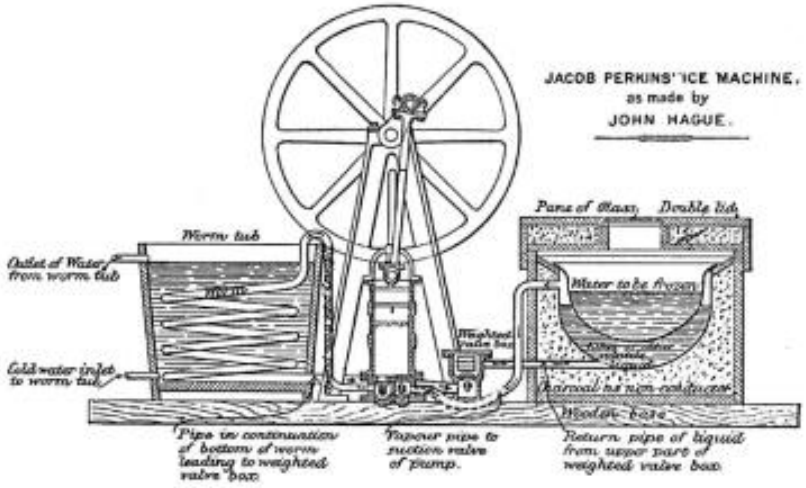

Figure 1.1 Perkin Ice Machine Built by January 20, 1883 [2].

In the mid-19th century, the field of cryogenics received a significant boost with the discovery of the first liquefied gases. Scientist Michael Faraday played a pioneering role in this development, successfully liquefying gases like ammonia, chloroform, and sulfur dioxide.

The origins of modern vapor-compression refrigeration systems, as we know them today, can be traced back to an 1834 British patent by Perkins, an American who had relocated to England. In this patent, Perkins, following Faraday's work, explained how the continuous liquefaction and expansion of gases could be achieved. This marked the beginning of the vapor-compression refrigerators we use today, as depicted in Figure 1.1. While the Perkins refrigerator was initially designed to

operate with ethyl ether, an actual refrigerator built by John Hague, as shown in Figure 1.1, used "caoutchoucine," a distillate of India rubber, which was readily available at the time, to produce small quantities of ice shortly after 1834.

A pivotal moment arrived in 1877 when Carl von Linde succeeded in liquefying oxygen, taking a major step towards reaching lower temperatures. This achievement set the stage for further advancements in cryogenics.

In 1888, James Dewar, one of the key figures in the history of cryogenic science, invented the first thermos, designed specifically for the storage of liquid hydrogen. This invention marked a practical application of cryogenic principles.

The year 1898 was a turning point in the field of cryogenics. Heike Kamerlingh Onnes successfully liquefied helium and, in the same year, made the groundbreaking discovery of superconductivity. This discovery opened the doors to both scientific and industrial applications of cryogenics, with superconductivity becoming a key area of research.

The 20^{th} century witnessed a surge in cryogenic science with the discovery and production of critical cooling agents such as liquid oxygen, liquid nitrogen, and liquid helium. These discoveries provided the necessary tools for a wide range of applications in fields like medicine, industry, space exploration, and research.

In the present day, cryogenic science plays a crucial role in modern medicine, industrial applications, space exploration, and scientific research. Liquid nitrogen and liquid helium have become indispensable for cooling and storage in laboratories and various industrial processes.

The development of cryogenic science has not only expanded our understanding of extremely low temperatures but has also opened up new frontiers in scientific exploration and technological advancements. Ongoing progress in this field promises a bright future for cryogenic science.

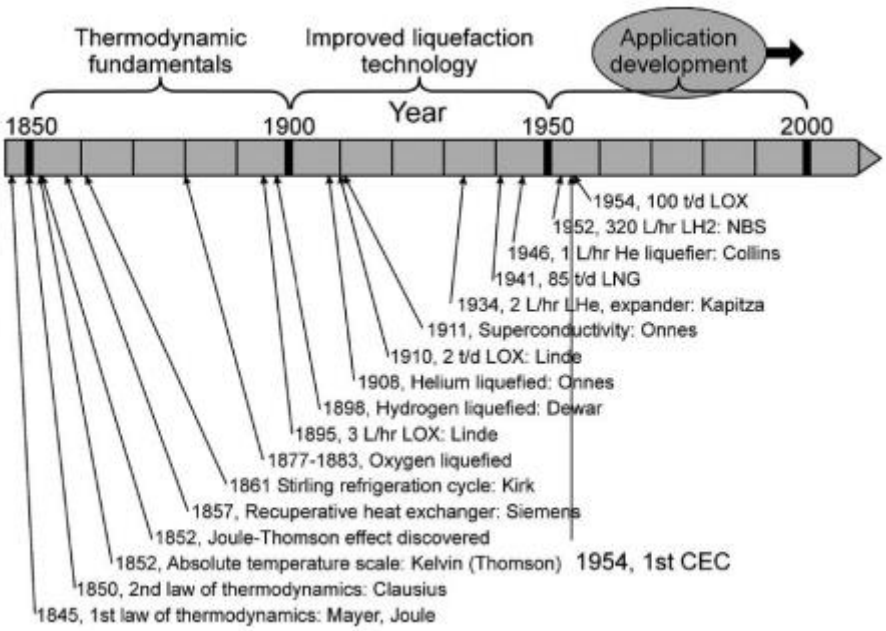

Figure 1.2 Illustrates the Century-Long Development of Cryogenics Between 1850 and 1950 [3].

1.2 Usage of Liquid Nitrogen in Cryogenic Applications

Liquid nitrogen, commonly symbolized as LN2, refers to nitrogen in a liquid state at extremely low temperatures. It has a boiling point of approximately -195.8 °C (-320 °F or 77 K). The industrial production of liquid nitrogen involves the fractional distillation of liquid air. It appears as a transparent and mobile liquid, with a viscosity roughly one-tenth that of acetone. Liquid nitrogen is particularly widely used as a coolant in various fields.

The N2 molecule maintains its two-atom structure even after being turned into a liquid. The limited interatomic attraction among N2 molecules is a result of the weak van der Waals interactions. This is what causes nitrogen to have an extraordinarily low boiling point. The temperature of liquid nitrogen can be easily brought down to its freezing point, which is -210 °C (-346 °F; 63 K), by placing it inside a vacuum chamber that has been evacuated using a vacuum pump. The efficiency of liquid nitrogen as a coolant is restricted by its immediate transformation into a gas upon contact with a warmer object. This results in the object being surrounded by an insulating layer of nitrogen gas bubbles. This phenomenon is known as the

Leidenfrost effect and happens whenever a liquid makes contact with a surface much hotter than its boiling point. To achieve quicker cooling, one can submerge an object in a mixture of both liquid and solid nitrogen, rather than using liquid nitrogen alone [4].

Table 1.1 Properties of Fluids Used in Cyrogenic Applications [5].

CRYOGEN	BOILING POINT (1 ATM) °C (°F)	CRITICAL PRESSURE PSIG“	LIQUID DENSITY, G/L	GAS DENSITY (27°C), G/L	LIQUID TO GAS EXPANSION RATIO
AR	-I86(-303)	710	1402	1.63	860
HE	-269(-452)	34	125	0.16	780
H_2	-253(-423)	188	71	0.082	865
N_2	-I96(-32I)	492	808	2.25	710
$O_;$	-!83(-297)	736	1410	1.4	875
CH_4	-161 (-256)	673	425	0.72	650

POUND PER SQUARE INCH GAUGE.

1.3 The Application of Cryogenic Liquids in Industrial Fields

Initially designed for the production of industrial gases, cryogenic cooling applications have expanded their scope to encompass a wide array of sectors, including military, space, medicine, energy, environment, transportation, agriculture, industrial, and commercial domains.

1.3.1 Gas Production and Refinement

Cryogenic cooling, a technology harnessed for its remarkable ability to achieve extremely low temperatures, finds extensive application in the intricate manufacturing and refining processes of industrial gases. Notably, substances like liquid nitrogen and oxygen, pivotal components in various industrial operations, benefit from the precision and efficiency that cryogenic cooling provides This method ensures the reliable production of high-quality industrial gases, contributing to a wide range of applications across industries such as healthcare, metallurgy, and manufacturing. The controlled and strategic implementation of cryogenic cooling in

this context underscores its critical role in enhancing the purity, efficiency, and overall reliability of the industrial gas production and refinement processes [6].

1.3.2 Food Industry

In the landscape of food production, the adoption of cryogenic cooling methods has emerged as a pivotal strategy. This technique utilizes extremely low temperatures to freeze, cool, and safeguard various food products, thereby contributing to the improvement of food quality and shelf life. Cryogenic cooling commonly involves using gases like liquid nitrogen or carbon dioxide at exceptionally low temperatures. These gases, known for their rapid evaporation at temperatures significantly below the ambient, serve as effective agents in the cooling processes within the food industry. The application of cryogenic cooling is particularly widespread in expansive food manufacturing plants and storage facilities, where a diverse range of products undergo freezing at reduced temperatures to ensure extended preservation.

One notable advantage of cryogenic cooling lies in its capacity to create smaller ice crystals within food products due to the rapid cooling process. This results in minimized damage to the cellular structure, leading to products of superior quality and freshness. Concerning production efficiency, the swift cooling attributes of cryogenic cooling can expedite production cycles, especially in high-volume manufacturing settings, thereby enhancing efficiency and reducing energy costs. While the benefits of cryogenic cooling are evident, ensuring its safe application is paramount. Additionally, the potential environmental impact of cryogenic cooling gases, with the capacity to harm the ozone layer, underscores the necessity for stringent controls in industrial applications to prevent uncontrolled emissions.

Cryogenic cooling distinguishes itself as an effective and versatile cooling method in the food industry. Its ability to meet vital industry demands, such as preserving quality, maintaining freshness, and extending storage periods, renders it a valuable technology. However, responsible utilization, considering safety and environmental considerations, is imperative for the sustainable integration of this technology into food production processes [7].

1.3.3 Medical Applications

Cryogenic cooling, the exploration of material behavior at extremely low temperatures, has become a cornerstone in modern medicine, offering diverse applications for various medical conditions. This technology, delving into the realms of cryotherapy, cryopreservation, cryosurgery, and cryonics, has demonstrated significant potential for enhancing medical treatments and interventions. In its simplest form, cryogenic cooling involves the study of materials and their properties at shallow temperatures. This discipline has evolved to find practical applications in medicine, with cryotherapy standing out as one of the most established methods. Cryotherapy, the application of extremely low temperatures for therapeutic purposes, has proven effective in alleviating pain and promoting healing. Cryopreservation, another key application, revolves around the controlled freezing of living structures and biochemical molecules. This process allows for the long-term storage of cells and tissues, ensuring their viability for future implantations. Notably, cryoprotectants play a crucial role in preventing cell destruction during this preservation process. Beyond preservation, cryogenic cooling has found its way into the field of cryosurgery. Here, extremely low temperatures are employed to eliminate damaged tissues or tumor cells. The precision and effectiveness of cryosurgery, especially in dermatology, make it a valuable tool for treating various benign and malignant conditions. Looking towards the future, cryonics introduces a concept where human cadavers are preserved at low temperatures with the hope of potential future revival. This speculative field envisions a synergy with nanotechnology, anticipating the regeneration or replication of damaged organs. In conclusion, the applications of cryogenic cooling in medicine are diverse and promising. From immediate pain relief through cryotherapy to the potential for future medical advancements in cryonics, this field continues to shape the landscape of modern medical science, offering new avenues for treatment, preservation, and potential breakthroughs [8].

1.3.4 Electronic Manufacturing

In the fast-changing world of electronics, the never-ending quest for better performance and efficiency has led to more and more challenges in dealing with

heat. As electronic devices get more complex, it's crucial to have good cooling systems. Cryogenic technology, usually used for various things, is now being considered as a new and innovative solution for electronic cooling. This article explores the principles, applications, advantages, and future possibilities of adding cryogenic cooling to electronic devices. Cryogenic cooling works by using extremely low temperatures to handle and get rid of the heat from electronic components. At these super low temperatures, materials undergo special changes, giving a chance to improve traditional ways of cooling electronics. There are many advantages to using cryogenic cooling in electronics, like better thermal conductivity and less energy usage. But, we need to recognize challenges such as complex systems and material compatibility to really understand how to use cryogenic cooling in electronics. Looking at where cryogenic technology is right now in electronic cooling gives us a good idea of what's happening and what people are researching. We can also guess about what might happen in the future, talking about potential improvements and changes. Cryogenic technology could make electronic systems more efficient and eco-friendly.

In the contemporary context, cryogenic technology, particularly in the cooling of electric vehicle batteries, holds the potential to enhance vehicular efficiency [9].

1.3.5 Astronomy and Space Research

Cryogenic cooling is an integral aspect of space telescopes and astronomical instruments, ensuring their optimal functioning at low temperatures.

1.3.6 Military Applications

The military sector extensively relies on the application of cryogenic cooling, which proves instrumental in various strategic and operational contexts. This cooling technology involves the use of devices and systems designed to operate at ultra-low temperatures, offering numerous advantages in military operations. The following points outline the key aspects of how cryogenic cooling is applied in military settings

Infrared Imaging Systems: Cryogenic cooling finds widespread use in thermal cameras and infrared imaging systems. These systems are pivotal for detecting and tracking enemy targets in conditions of low visibility.

Laser Technologies: Military laser systems benefit from cryogenic cooling to maintain optimal performance. This cooling method effectively manages the heat generated by laser systems, contributing to enhanced targeting capabilities over longer distances.

Electronic Devices and Communication Equipment: Cryogenic cooling is implemented in the cooling processes of diverse electronic devices used in military aircraft and naval vessels. This ensures the smooth operation of electronic equipment at higher frequencies and for extended durations.

Missile Systems: Cryogenic cooling is employed to store fuel, thereby enhancing the overall performance of missile systems. It also facilitates the preservation of sensitive equipment within missile warheads by maintaining low temperatures.

Space Exploration and Defense: Cryogenic cooling plays a crucial role in optimizing the functionality of space-based systems. Space telescopes and exploration equipment benefit from the precision offered by low-temperature operations. For example a cryogenic rocket engine is an innovation in space exploration, utilizing cryogenic fuel and oxidizer—both gases liquefied and stored at extremely low temperatures. These advanced engines, first utilized on the US Atlas-Centaur, played a crucial role in NASA's successful lunar missions with the Saturn V rocket. The application of cryogenic technology has not only showcased exceptional efficiency but has also been a defining factor in shaping significant milestones in the history of space exploration.

Chemical and Biological Threat Detection Systems: Cryogenic cooling contributes to the development of more sensitive detection systems for military units, especially in countering chemical and biological threats.

The deployment of cryogenic cooling in military applications ensures technological superiority, increased operational ranges, and heightened precision in detection systems. Consequently, it is a fundamental component of military defense and intelligence operations [10].

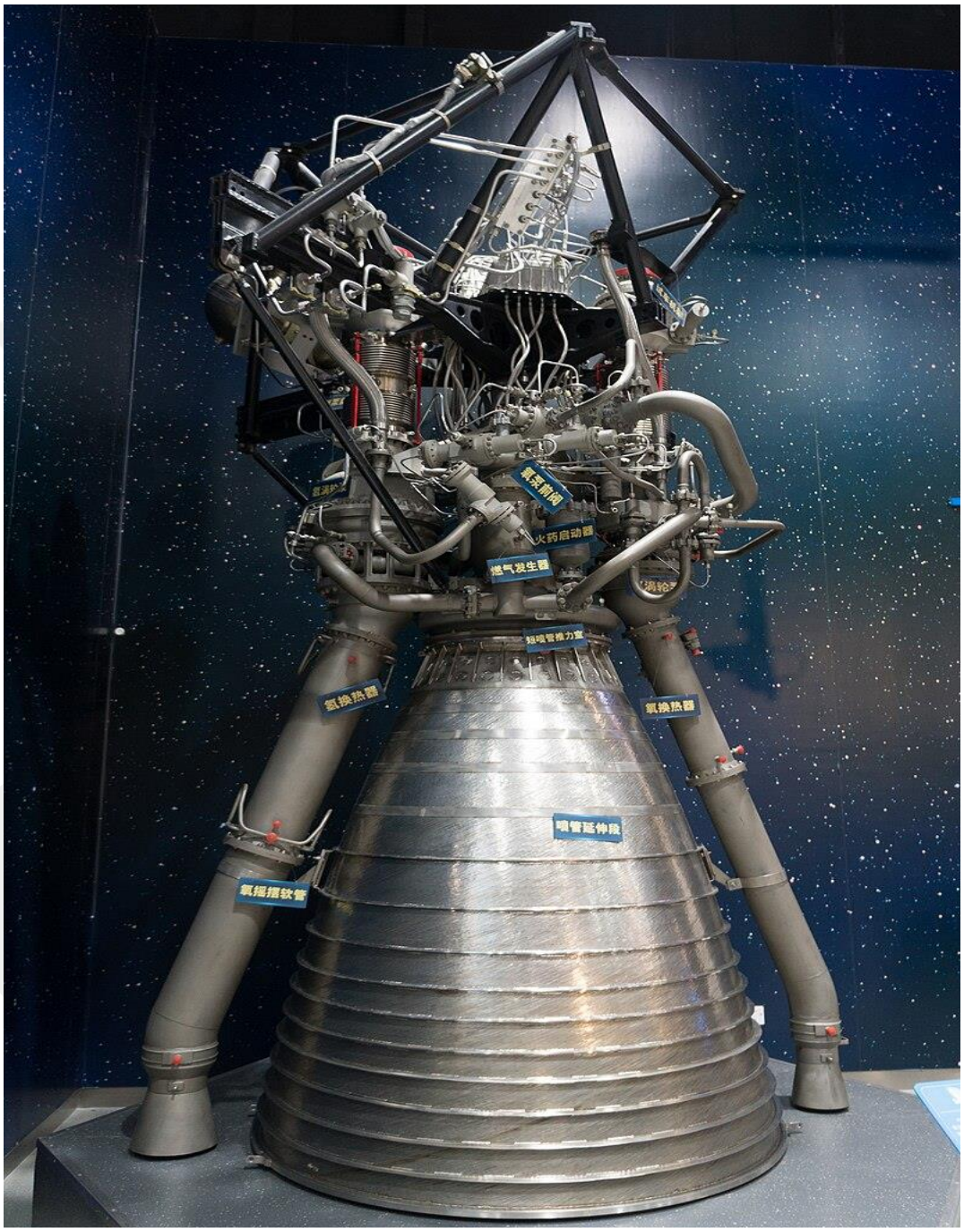

Figure 1.3 Chinese YF-77 Engine Used by Long March 5 [11].

1.3.7 Scientific Study Applications

The recent development of cryogenic science has spurred numerous contemporary scientific investigations in this field. Furthermore, the utilization of cryogenic temperatures serves as the foundational technology for various ongoing scientific studies in other disciplines. Presently, cryogenic science plays a crucial role in the widely acclaimed Hadron colliders. The Large Hadron Collider, a 27 km circumference collider employed at CERN (European Organization for Nuclear Research), incorporates a multitude of NbTi dipole magnets (Figure 2.4). Operating at a temperature of 1.9 K, these magnets generate an exceptionally high magnetic field, facilitating the acceleration of hadrons (subatomic particles). The operational temperatures of these magnets fall within the purview of cryogenic science [12].

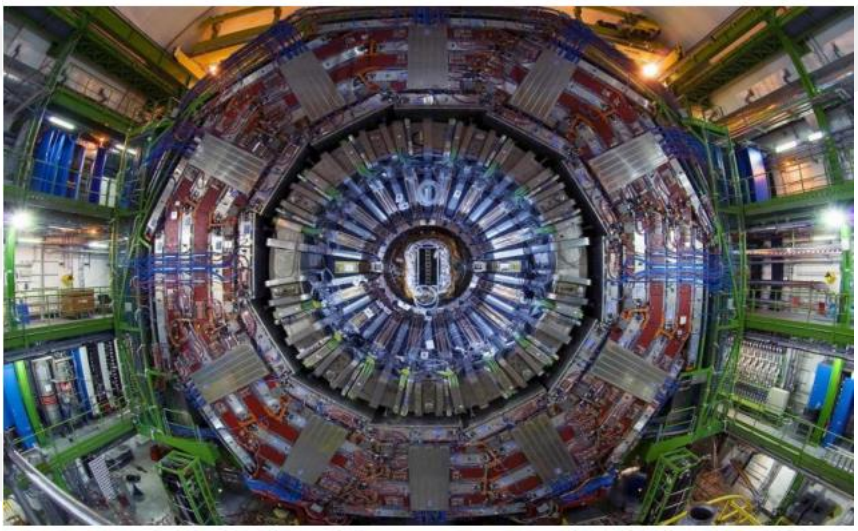

Figure 1.4 CERN Hadron Collider [13].

This thesis adopts a unique perspective by delving into a distinct design and implementation approach for cryogenic cooling, diverging from the general application areas of cryogenic cooling. The highlighted specific design features in the thesis elucidate how cryogenic cooling technology can be optimized within a specific context. The study suggests that, beyond existing designs, there is potential for enhancing the application areas of cryogenic cooling for numerous specific applications.

CHAPTER 2

LITERATURE SURVEY

In their research, Loránd Szabó and his colleagues [14], provide a succinct overview of superconducting machines, offering explanations of various technologies utilized in the context of cryogenic motors and generators. They specifically delve into topics such as cooling systems, cryogenic fluids, and materials applied in cryogenic electrical machines.

Furthermore, the authors outline prospective research directions for the forthcoming years and elucidate the landscape of electric machines employing cryogenic cooling.

In a broader context, this article serves as a guide for engineers and designers, facilitating their comprehension of the methodologies and materials used in cryogenic electric motors while enabling them to evaluate the potential of this technology. Additionally, it contains concise information on the thermodynamics and practical applications of cryogenic fluids.

In another study Efstratios Tsolakis and his colleagues [15], a cooling chamber was designed for concrete samples measuring 150 mm in diameter and 300 mm in height to determine the coefficient of thermal expansion of concrete at low temperatures using liquid nitrogen cooling. Two thermocouples were placed on the chamber's walls at a distance of 10 mm from the surface, and one thermocouple was positioned at the center. Pressure losses in the cooling coil were calculated using Darcy's laws. Three concrete samples were thermally tested under controlled conditions, cooled from 0°C to -160°C using a cryogenic cooling system with liquid nitrogen, and then reheated to 0°C. As a result, changes in the coefficient of thermal expansion of concrete were examined through the use of the cryogenic cooling system with liquid nitrogen.

In their study, Khan, A.A., and Ahmed, M.I. [16], examined the use of cryogenic cooling to increase the tool life of cutting tools. With cryogenic cooling, they sprayed liquid nitrogen onto the workpiece at temperatures below -150°C during machining processes and analyzed the results. This cooling method yielded various beneficial outcomes in machining operations, including the extension of tool life, improvement in surface quality, and reduction in cutting forces. Furthermore, they indirectly demonstrated the highly efficient cooling capabilities of cryogenic liquids, such as liquid nitrogen, even in extremely short durations.

The study issue of Dhar [17] and friends examined the utilization of cryogenic cooling in metal machining processes. Their research emphasized the efficiency and environmental benefits of cryogenic fluids in contrast to conventional lubricants, which are known to contribute to environmental pollution. The findings of Dhar support the study conducted by Khan, A.A., and Ahmed, M.I. (2008) and underscore the viability of cryogenic cooling as a more environmentally friendly and efficient alternative in metalworking operations.

In a study by Xue (2022) [18], a small wind tunnel prototype was constructed using liquid nitrogen spray cooling to understand the performance of multi-nozzle spray cooling. The transient and steady-state cooling performance was experimentally examined. According to the findings of this study, as the spraying rate of liquid nitrogen decreases, the cooling rate increases, while an increase in the number of nozzles and the pressure of liquid nitrogen enhances the cooling rate.

In the work conducted by Jacobs (1963) [19], the constraints on cryogenic liquid consumption were thoroughly examined and presented graphically. According to this research, the consumption of cryogenic liquid in the cooling process of equipment is directly linked to the change in enthalpy of the equipment's cold mass. It is also inversely proportional to the sum of the liquid's latent heat and a portion of the sensible heat of the vaporized gas. The primary objectives of this paper are threefold:

To establish equations that facilitate the estimation of cryogenic liquid consumption to calculate the cooling requirements for commonly used cryogenic liquids (helium, hydrogen, nitrogen, and oxygen) with respect to commonly used materials (stainless

steel, copper, and aluminum). To present the computational results in an easily interpretable graphical format.

This study is founded upon two pivotal limits for liquid consumption, which are instrumental in determining the necessary liquid quantity for the cooling process of equipment;

Minimum liquid requirement: This signifies the minimum amount of liquid required when a cryogenic liquid operates a system, utilizing its entire cooling capacity. Essentially, it is equal to the enthalpy change of the liquid.

Maximum liquid requirement: In contrast, this represents the maximum amount of liquid required when a system is cooled using solely the latent heat of the liquid and the sensible heat of the vaporized gas.

These limits serve to define the boundaries of cryogenic liquid consumption and aid in comprehending the necessary liquid volume under different operating scenarios.

Zong (2021) [20] study, inspired by Jacobs' (1963) work, a continuous factor (α) varying between 0.0 and 1.0 is introduced to quantify the utilization of sensible heat alongside latent heat. This factor is treated as an independent variable in the calculation of specific liquid requirements. Specific liquid requirements for different α values are computed to bridge the gap between the minimum and maximum requirements.

The study demonstrates a decreasing trend in specific liquid requirements with the increasing utilization of sensible heat, especially when cooling processes involve cryogenic liquids with high sensible heat, such as liquid helium and liquid nitrogen. Additionally, it provides thermal properties of commonly used materials.

This research offers valuable insights for a better understanding and optimization of the use of cryogenic liquids in cooling processes.

In A. Hofman's 2006 study [21], an empirical function is proposed for analyzing the thermal conductivity of cryogenic insulation materials and calculating their integral

mean values. This function allows experimentally obtained values to be extrapolated to different temperature levels. The selection of materials in the study covers granulated and fibrous insulations under both atmospheric pressure and vacuum conditions, as well as a multilayer insulation designed for high-performance applications. The study also theoretically demonstrates how to determine the constants in the empirical function, and their practical calculation is shown using real measurement data. For multilayer insulation, a theory is developed that enables the extrapolation of measured values to various temperatures, gas pressures, and numbers of insulation layers. The application of this theory to a real insulation system is also illustrated. The study's findings and results are presented in a tabular summary.

In his study, Feshmire (2015) [22] focused on the advancements in cryogenic insulation test apparatus and methods. He examined various techniques as outlined in two new technical standards from ASTM International, namely C1774- Standard Guide for Thermal Performance Testing of Cryogenic Insulation Systems and C740 - Standard Guide for Evacuated Reflective Cryogenic Insulation. Among these techniques, he provided a detailed analysis of the cylindrical boil-off calorimeter, which allows for absolute heat measurement over the full range of vacuum pressure conditions.

This apparatus and test method are particularly valuable for assessing the thermal performance of different multilayer insulation (MLI) systems, which are commonly used in cryogenic applications to minimize heat transfer. The study included benchmark thermal performance data, including measures like effective thermal conductivity (ke) and heat flux (q). These data covered a range of MLI systems and were compared with the performance of other commonly used insulation systems such as perlite powder, fiberglass, polyurethane foam, and aerogels. The results offered insights into the effectiveness of various insulation materials and techniques, which is crucial for the design and optimization of cryogenic systems operating at different temperature boundaries, particularly at 293 °K and 77 °K.

Upon reviewing the literature, limited data has been found regarding the use of cryogenic cooling for similar applications. Examining publications in this field reveals a lack of similar applications on such a significant scale. The heating and cooling system, cabin static design, and analysis methods studied in this thesis have not been encountered in the literature in any comprehensive study. However, given its uniqueness in terms of application and approach, this study can serve as an exemplary work for future research in similar areas. The existing methods are open to further development and diversification.

CHAPTER 3

DESIGN METODOLOGY AND CALCULATIONS

In this chapter, the problem has been defined, and boundary conditions have been established. The mathematical solution method for the problem has been determined. Necessary assumptions and the methods to be employed for the solution have been elaborated in detail.

3.1 Problem Statement and Requirements

The primary design considerations for the cabinet stem from its multifunctional use in testing various aviation equipment. Commencing with preliminary design processes involves selecting key dimensions and conducting heating and cooling load calculations. Given that the largest aviation equipment to undergo testing weighs 500kg, with dimensions of 1200 mm in width, 4600 mm in length, and 800mm in height, the initial design dimensions, excluding insulation, are set to be larger than these specifications. Thus, the preliminary design is established with internal dimensions of 1200 x 4600 x 800 mm.

3.1.1 Coolant Types and Calculation Equations for Determining the Required Coolant Amount

Cryogenic liquids are specialized substances that exist in either gaseous or liquid states at temperatures typically below -150°C. Among these liquids are nitrogen (LN2), liquid oxygen (LOX), liquid hydrogen (LH2), neon, and others.

Understanding the thermodynamic properties of these liquids, such as latent heat, specific heat, and enthalpy values, is crucial for comprehending and optimizing their

performance in specific applications. Latent heat represents the energy exchange during temperature variations in these liquids. Specific heat denotes the energy change per unit mass, while enthalpy expresses the total energy in a system as a sum of internal energy, pressure, and volume.

For instance, in industrial and medical fields, cryogenic liquids find applications in low-temperature storage, material preservation, medical procedures, and space exploration. The thermodynamic properties of these liquids play a critical role in ensuring energy efficiency and safety during processes such as storage, transportation, and utilization. Table 3.2 provides the thermodynamic properties of the liquids.

Therefore, a profound understanding of the thermodynamic characteristics of cryogenic liquids is essential for optimizing and enhancing their utilization across various industrial and scientific applications. This knowledge contributes to the improvement of energy efficiency and safety in the storage, transportation, and application of these liquids.

Table 3.2 Properties of Fluids Used in Cyrogenic Applications [23].

		Liquid at normal boiling point				Vapor at $1.013x10^5$ Pa (1 atm)			
Fluid	Atomic	Temp.	Density	Enthalpy	Spec. hl.	Temp.	Density	Enthalpy	Spec. hi.
	mass				f p				c_p
	u	K	mol.'L	J/mol	J/(molK)	K	mol/L	J/mol	J/(molK)
Helium	4.0026	4.222	31.20	-21.0	21.10	4.222	4.226	62	36.73
						20.27	0.601	419	21.01
						27.09	0.449	562	20.91
						77.37	0.157	1609	20.80
						90.20	0.135	1876	20.79
						273.15	0.045	5679	20.79
Hydrogen	2.0159	20.27	35.12	-516	19.49	20.27	0.664	382	24.68
						27.09	0.471	539	22.15
						77.37	0.158	1632	23.36
						90.20	0.135	1944	25.38
						273.15	0.045	7657	30.36
Neon[1,]	20.180	27.09	59.71	-1203	38.8	27.09	0.476	525	24.1
						77.37	0.158	1602	20.9
						90.20	0.135	1869	20.9
						273.15	0.045	5676	20.8
Nitrogen	28.134	77.37	28.86	-3401	57.79	77.37	0.165	2164	31.45
						90.20	0.139	2559	30.43
						273.15	0.045	7934	29.15
Oxygen	31.999	90.20	35.66	-4263	54.22	90.20	0.140	2535	31.35
						273.15	0.045	7937	29.33

■ 'NIST Standard Database 12: NIST Thermophysical Properties of Pure Fluids, (Version 3.0). D. G. Friend (NIST. Gaithersburg. MD. 1992).

The required amount of liquid for cooling was determined with reference to the study titled "Jacobs, R. B. (1963) [24]. Cryogenic Liquid Consumption: Limits and Estimation." The experimental equations derived in Jacobs' study were modeled and applied in a manner compatible with the system used in this study.

The system requirements include a cooling system capacity that can cool a payload of at least 1000kg without the need for refilling.

Before performing these calculations, certain assumptions will be made. These include the assumption that liquid nitrogen is at its saturation temperature, namely, at -196°C, and not below this temperature. This allows the consideration that heat transfer occurs only through latent heat. Additionally, it is assumed that the liquid nitrogen tank and the equipment conveying nitrogen to the cabin are adiabatic with the external environment. Furthermore, the cabin is assumed to be well-insulated and treated as adiabatic.

Consider the interaction between a small quantity of fluid (dmf) and a small quantity of equipment (dme). Before the interaction, the temperature of the equipment is Te, and after the interaction, it reaches (Te + dTe). The fluid is in a saturated liquid state before the interaction, but post-interaction, the fluid's temperature is (Tf + dTf). In reality, the equipment doesn't cool uniformly as assumed. However, as long as the fluid departs the system at a temperature equal to the warmest part of the equipment, any disparities between the analytical model and the actual process don't impact these energy calculations.

The heat transfer to the equipment during the interaction is;

$$\delta\theta_e = +dC_e\, dT_e \qquad \text{(Eqn. 3.1)}$$

Where Ce is the specific heat of the equipment. The heat transfer to the fluid during the interaction is;

$$\delta\theta_f = dm_f\,[\lambda + \int_{T_s}^{T_e} C_{pf}\, dT_f\,] \qquad \text{(Eqn. 3.2)}$$

Where λ is the latent heat of vaporization of the liquid, Cpf is the isobaric specific heat of the vapor, T. is the saturation temperature of the fluid, and Tf is the temperature of the fluid. It has been assumed that dT_e is negligible compared with T_e and that the interaction is isobaric.

Substituting the above expressions into;

$$\delta\theta_e = -\delta\theta_f \qquad \text{(Eqn. 3.3)}$$

and rearranging, we obtain;

$$dm_f = -dm_e\, C_e \left[\lambda + \int_{T_s}^{T_e} C_{pf}\, dT_f\right]^{-1} dT_e \qquad \text{(Eqn. 3.4)}$$

When integrating, we derive the formula representing the quantity of liquid needed to cool a mass of equipment, denoted as dme, from an initial temperature T_a to a final temperature T_c:

$$m_f = d\, m_e \int_{T_s}^{T_e} \left(C_e \left[\lambda + \int_{T_s}^{T_e} C_{pf}\, \partial T_f\right]^{-1}\right) d\, T_e \qquad \text{(Eqn. 3.5)}$$

The initial and final temperature of systems are not uniform for that an additinal integral operator calculated:

$$m_f = \int_{m_e} \int_{T_s}^{T_e} \left(C_e \left[\lambda + \int_{T_s}^{T_e} C_{pf}\, \partial T_f\right]^{-1}\right) d\, T_e\, d\, Tm_e \qquad \text{(Eqn. 3.6)}$$

This integral is performed over the entire mass of the system m_e and requires knowledge of the temperature distribution throughout the system. It should be noted that if the system is composed of various materials, the specific heat C_e must be considered accordingly. We assume that a complex system can be divided into components that are homogeneous in composition and have uniform initial and final temperatures. In this case, the liquid required to cool a complex system is simply the sum of the requirements for each component piece. Therefore, for each mass component Δm_e, we have the following integral:

$$m_f = \Delta m_e \int_{T_s}^{T_e} (C_e \left[\lambda + \int_{T_s}^{T_e} C_{pf}\, \partial T_f \right]^{-1}) \, d\, T_e \qquad \text{(Eqn. 3.7)}$$

The "specific liquid requirement," denoted as ϭ, represents the amount of liquid needed to cool one unit of equipment mass from an initial temperature T_a to a final temperature T_e. This parameter will be consistently used in the following discussion. The mass of liquid required to cool a specific equipment component is simply the product of the specific liquid requirement and the mass of that equipment piece.

The minimum specific liquid requirement, $ϭ_{min}$, is expressed as:

$$ϭ_{min} = \int_{T_s}^{T_e} (C_e \left[\lambda + \int_{T_s}^{T_e} C_{pf}\, dT_f \right]^{-1}) \, d\, T_e \qquad \text{(Eqn. 3.8)}$$

The specific heat change of nitrogen vapor from zero to its boiling point is less than $1.5\, J/mol.K$ and shows negligible variation with temperature. Therefore, Equation (3.8) can be simplified as follows

$$ϭ_{min} = \int_{T_s}^{T_e} (C_e \left[\lambda + C_{pf}(T_e - T_{e\,s}) \right]^{-1}) \, d\, T_e \qquad \text{(Eqn. 3.9)}$$

The average specific heat of the equipment is utilized,

$$ϭ_{min} = \frac{C_e}{C_{pf}} In \left[\frac{1+(\frac{C_{pf}}{\lambda})(T_a - T_s)}{1+(\frac{C_{pf}}{\lambda})(T_c - T_s)}\right]^{-1}) \, d\, T_e \qquad \text{(Eqn. 3.10)}$$

We write the equation 8 for $T_c \neq T_s$ it is become;

$$ϭ_{min} = \int_{T_s}^{T_a} (C_e \left[\lambda + \int_{T_s}^{T_e} C_{pf}\, dT_f \right]^{-1}) \, d\, T_e - \int_{T_s}^{T_c} (C_e \left[\lambda + \int_{T_s}^{T_e} C_{pf}\, dT_f \right]^{-1}) \, d\, T_e$$

(Eqn. 3.11)

By using Jasons Specific curve of liquid-nitrogen requirement for cool-down as a function of initial equipment temperature (Table 3.3) the function written as;

$$ϭ_{min} = ϭ_{min}|_{T_s}^{T_a} - ϭ_{min}|_{T_s}^{T_c} \qquad \text{(Eqn. 3.12)}$$

The liquid required to cool equipment from any temperature T_a to any temperature T_c ($\geq T_s$,) can be computed from (Eqn 3.12) and.

Table 3.3 Specific Liquid-Nitrogen Requirement for Cool-Down as a Function of Initial Equipment Temperature.

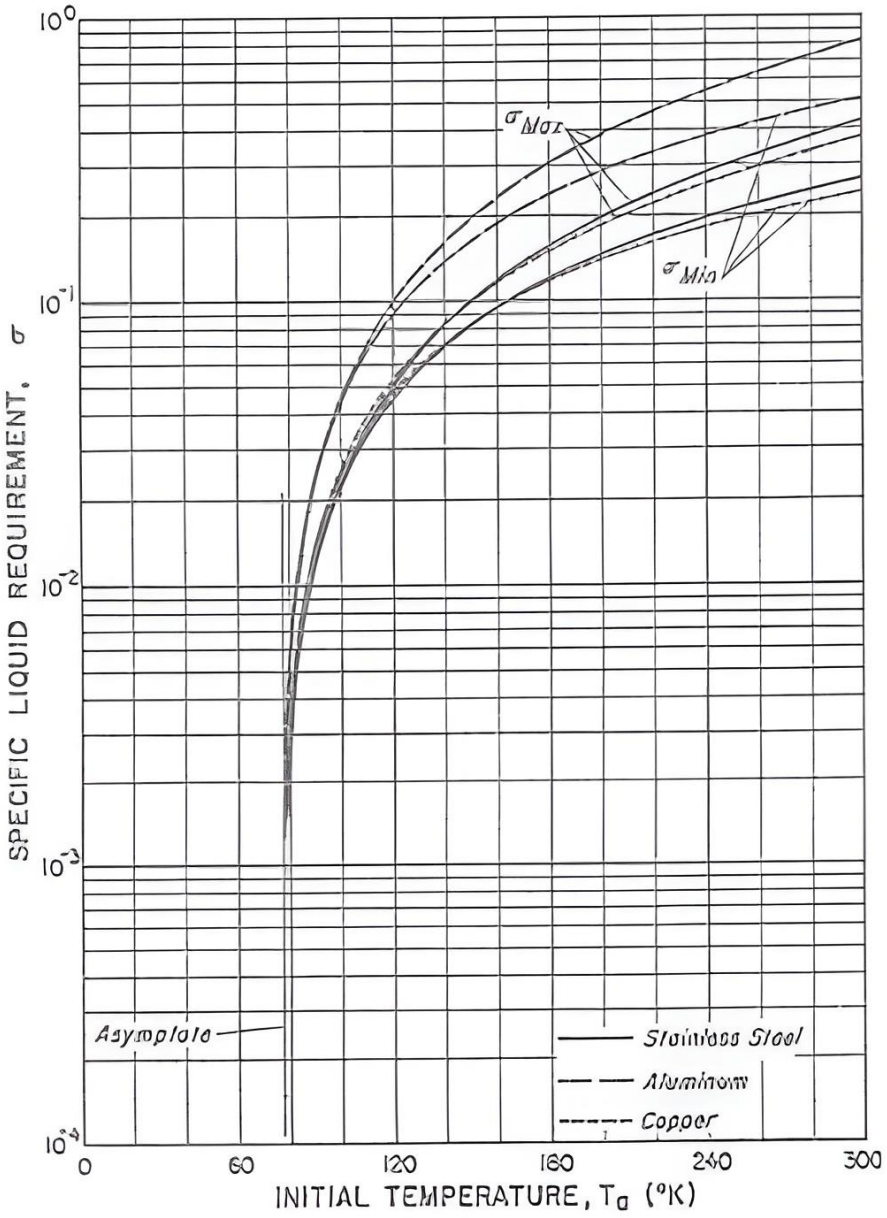

3.1.2 Cooling of Existing Air in Chamber

Inside the cabin, there will be metal along with air. The characteristics of this air are assumed for Ankara conditions at an elevation of 997 meters with a maximum humidity of 60%. Nitrogen will be sprayed into the cooling chamber in the form of saturated nitrogen. Therefore, the mixture temperature is assumed to be -196°C. The system is closed and insulated, so heat transfer is considered adiabatic.

The ideal gas properties of air are provided in Table 3.4. Additionally, in Table 3.5, a psychrometric chart has been drawn in accordance with the SI unit system.

$$m_{air} = \frac{R.T}{P.V} \quad \text{(Eqn. 3.13)}$$

$$m_1 C_1 \, \Delta T_1 = m_2 \, C_2 \, \Delta T_2 \quad \text{(Eqn. 3.14)}$$

Table 3.4 Ideal Gas Specific Heats of Some Common Gases [25].

Temp. K	c_p	c_v	k	c_p	c_v	k	c_p	c_v	k	Temp. K
	Air			Nitrogen. N			Oxygen			
250	1.003	0.716	1.401	1.039	0.742	1.400	0913	0.653	1.398	250
300	1.005	0.718	1.400	1-039	0.743	1.400	0.918	0.658	1-395	300
350	1.008	0.721	1.398	1.041	0.744	1-399	0.928	0.668	1.389	350
400	1.013	0.726	1-395	1-044	0.747	1-397	0.941	0.681	1.382	400
450	1.020	0-733	1.391	1049	0.752	1-395	0956	0.696	1-373	450
500	1.029	0.742	1.387	1.056	0.759	1.391	0.972	0.712	1-365	500
550	1.040	0-753	1.381	1.065	0.768	1.387	0.988	0.728	1.358	550
600	1.051	0.764	1.376	1-075	0.778	1.382	1.003	0-743	1.350	600
650	I.O63	0.776	1.370	1.086	0.789	1.376	1.017	0.758	1-343	650
700	1.075	0.788	1.364	1.098	0.801	1-371	1.031	0.771	1-337	700
75°	I.O87	0.800	1-359	1.110	0.813	1.365	1-043	0.783	1.332	750
800	I.O99	0.812	1-354	1.121	0.825	1.360	1054	0-794	1-327	800
900	1.121	0.834	1-344	1-145	0.849	1-349	1074	0.814	1.319	900
1000	1.142	0.855	1.336	1.167	0.870	1-341	1.090	0.830	1.313	1000

Table 3.5 Psychrometric Chart for 1 atm (SI units) [26].

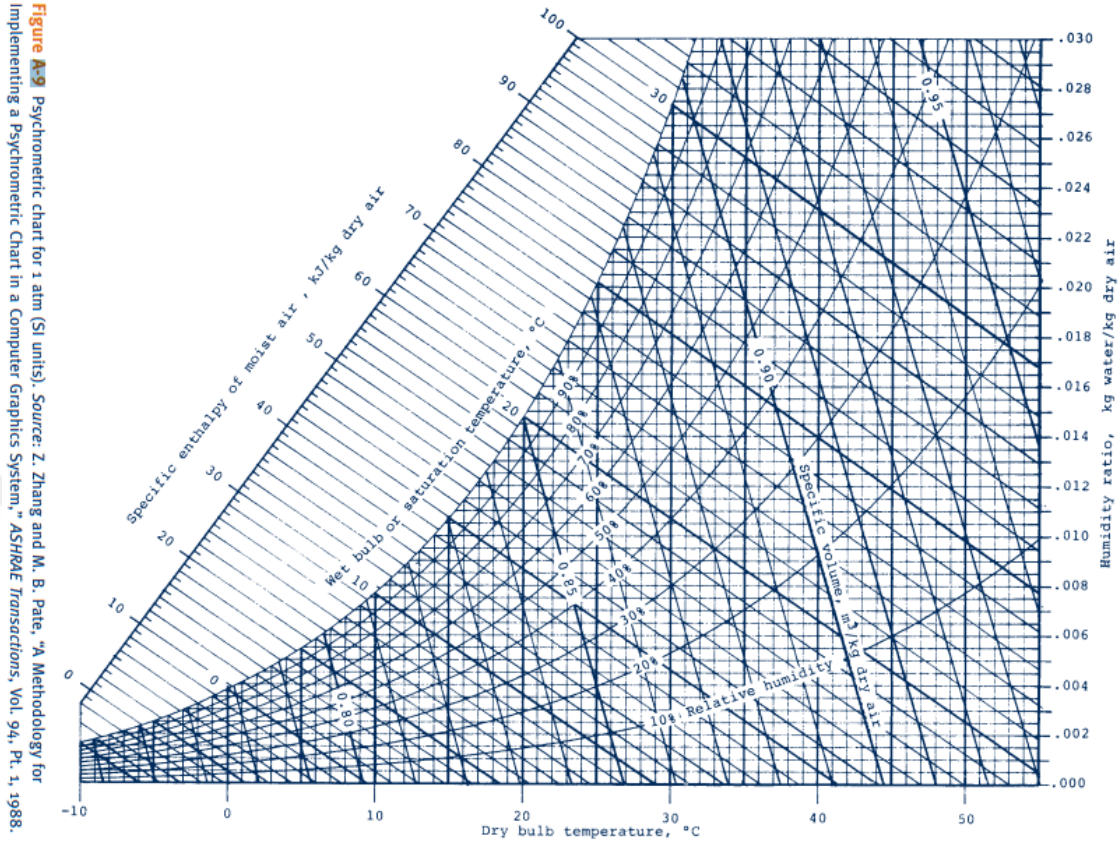

Figure A-9 Psychrometric chart for 1 atm (SI units). *Source:* Z. Zhang and M. B. Pate, "A Methodology for Implementing a Psychrometric Chart in a Computer Graphics System," *ASHRAE Transactions*, Vol. 94, Pt. 1, 1988.

3.1.3 Insulation Thickness and Insulation Materials

The requirement for thermal conductivity of 8 $\frac{W}{m^2}$ is a critical pre-design specification, aligning with recommendations from insulation material manufacturers such as Izocam [27].

Internal and external temperatures have been set at -55°C and 25°C, respectively, resulting in an 80°C temperature difference, as previously established for determining the quantity of liquid nitrogen. The thermal conductivity table recommended for cold rooms in ASHRAE 2018 has been included for reference. To ensure accuracy, results obtained through manual calculations have been cross-verified using the Izocam insulation program.

The insulation thickness of the cabin was calculated using the available thermal conductivity coefficient. The effects of conduction and radiation on heat transfer were considered negligible. The cabin was assumed to be adiabatic, and calculations were based on the critical cooling load, considering that the cooling load is greater than the heating load. Heat transfer was assumed to be in a continuous and time-independent steady-state regime.

For the process, the heat transfer resistance of composite walls was initially calculated, and it was observed to be below the value in the ASHRAE table.

$$R_{Total} = \frac{e_1}{\lambda_1} \quad \text{(Eqn. 3.15)}$$

$$\sum \mathrm{R}_{TOTAL} = \frac{e_1}{\lambda_1} + \frac{e_2}{\lambda_2} + \frac{e_3}{\lambda_3} \quad \text{(Eqn. 3.16)}$$

$$\varphi = \frac{\theta}{A} = \frac{(T_{in} - T_{out})}{R_{TOTAL}} \quad \text{(Eqn. 3.17)}$$

$$\varphi = \frac{\theta}{A} = \frac{(T_{in} - T_{out})}{R_{TOTAL}} \quad \text{(Eqn. 3.18)}$$

$$\theta = \varphi \; x \; A \quad \text{(Eqn. 3.19)}$$

Table 3.6 2018 ASHRAE Handbook - Refrigeration, Chapter 23-Recommended Thermal Resistance for Cold Rooms [28].

Type of Facility	Temperature Range, °F	Thermal Resistance R, °F ft^2 h/Btu		
		Floors	Walls/Suspended Ceilings	Roofs
Coolers	40 to 50	Perimeter only	25	30
Chill coolers	25 to 35	20	25	35
Holding freezer	-10 to-20	27	35	45
Blast freezer	-40 to -50	30	45	50

In cold room insulation, commonly used materials include EPS (Expanded Polystyrene), XPS (Extruded Polystyrene), and mineral wool. These materials help reduce heat transfer in cold environments due to their low thermal conductivity.

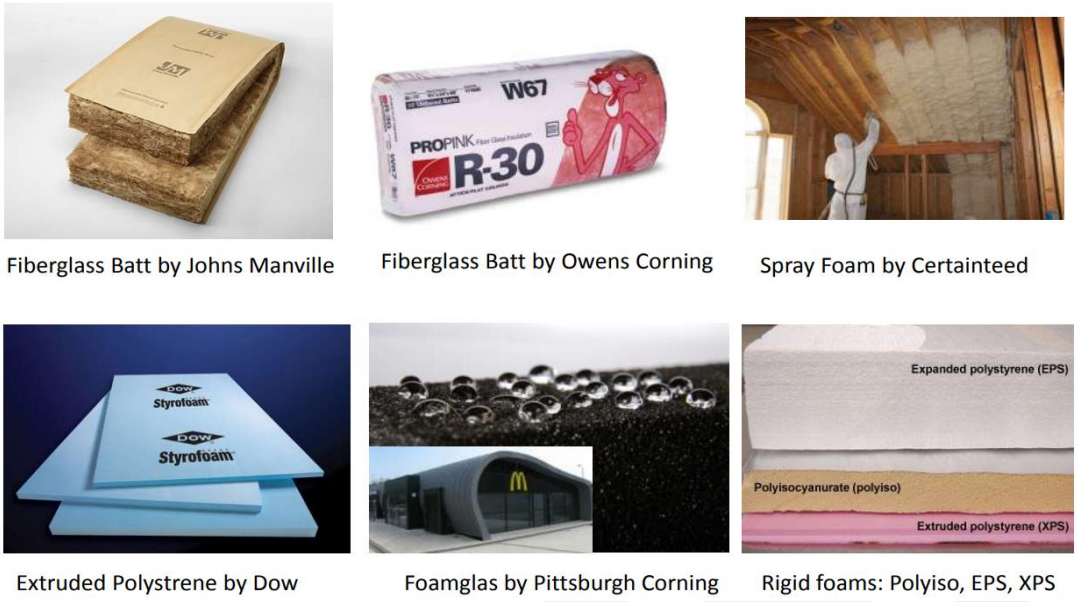

Figure 3.5 Cold Room Insulation Materials [29].

In cryogenic applications, materials resistant to lower temperatures are typically used. Among these materials are specially developed foam materials, Vacuum Insulation Panels (VIPs), multi-layer insulation materials, and superconducting materials. The R-value, indicating thermal resistance, of cryogenic insulation materials is usually designed to be more effective at lower temperatures.

Table 3.7 Thermal Insulatıng Performance in R-Value of Varıous Materıals [29].

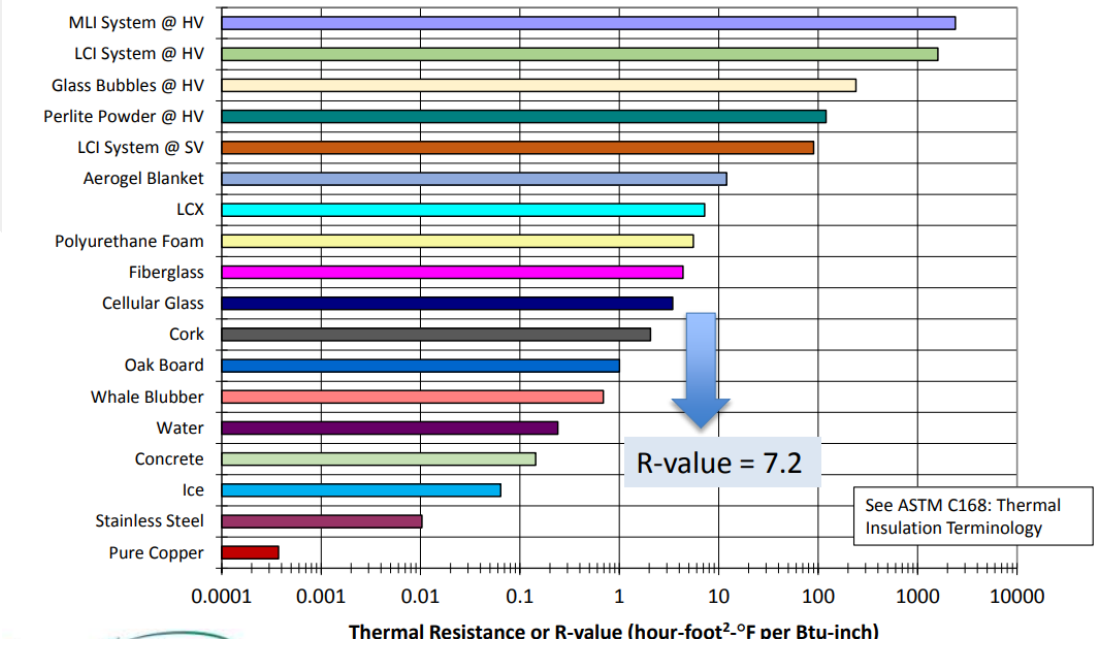

Figure 3.6 Polyurethane Foam Application [30].

3.1.4 Heating Capacity Calculation Metodology

Electric heaters are used for the heating process of the cabin. This section explains the assumptions and methods employed for the selection of electric heaters. The required power to raise the temperature of the air inside the cabin from 25 degrees to 70 degrees has been calculated. In these calculations, the relatively low heat loss has been neglected. The system is considered as an adiabatic system. The power required to heat the metal is assumed to be much less than the power required to heat the air, so the air is treated as dry air, and the humidity level is neglected. This is because the mass of the air to be heated is much smaller compared to the mass of the metal.

The energy required to heat the air has been calculated using Equation 3.20. The enthalpy values for two different temperatures of the air have been obtained from the thermodynamic table, multiplied by the total air mass, and the necessary energy has been determined in kilojoules. The energy required to heat the metal, on the other hand, has been calculated using Equation 3.21.

$$\emptyset = m(h_2\text{-}h_1) \quad \text{(Eqn. 3.20)}$$

$$\emptyset = m\ c\ \Delta_t \quad \text{(Eqn. 3.21)}$$

Where:

- ∅ represents the heat energy (joules),
- m represents the mass (kilograms),
- c represents the specific heat capacity (joules per gram per Kelvin),
- ΔT represents the temperature change (in Kelvin).

Figure 3.7 Electric Resistors With a Power Of 2 kW.

3.1.5 Structural Design of the Cabin

In the cabin design, one of the most crucial factors is corrosion resistance and weight. The inner chassis of the cabin needs to be selected from a material resistant to corrosion since it will be directly exposed to corrosive phase change processes and fluids such as liquid nitrogen. Additionally, considering that the inner chassis will bear the entire load, sheet thicknesses should be at appropriate values. As for the outer chassis of the cabin, it only serves as a shell connecting the inner chassis with insulation, so it can be chosen from a readily available industrial product. The

components connecting the inner and outer chassis should have low thermal conductivity. Simultaneously, they must be made of a material capable of withstanding high stresses, sufficient to support the weight of the cabin in accordance with design requirements.

The material selection and corresponding calculations are comprehensively outlined in the sections titled "Structural Design of the Cabin" and "Structural Design Analysis of the Cabin."

This comprehensive design approach ensures that the cabin meets the stringent requirements of accommodating diverse aviation equipment testing, ensuring structural integrity, and facilitating effective cooling during the testing processes.

3.1.6 Structural Materials

In this section, details related to the materials used in structural design are provided.

3.1.6.1 Stainless Steels

The chromium-nickel-molybdenum austenitic stainless steel, known as alloy 316/316L (UNS S31600/S31603), was developed to enhance corrosion resistance compared to Alloy 304/304L, especially in environments with moderate corrosion levels. This alloy is commonly employed in processing streams containing chlorides or halides. The addition of molybdenum significantly improves both general corrosion resistance and resistance to chloride pitting. Furthermore, it imparts heightened creep, stress-to-rupture, and tensile strength at elevated temperatures.

A standard practice involves dual certification of 316L as both 316 and 316L. The low carbon content of 316L, coupled with an addition of nitrogen, enables it to meet the mechanical properties of 316. Alloy 316/316L exhibits resilience against atmospheric corrosion and performs well in moderately oxidizing and reducing environments. It also withstands corrosion in polluted marine atmospheres and demonstrates remarkable resistance to intergranular corrosion in the as-welded condition. This alloy maintains exceptional strength and toughness even at cryogenic temperatures.

In the annealed state, Alloy 316/316L is non-magnetic, although it may acquire slight magnetism due to cold working or welding. The alloy is easily weldable and can be processed using standard shop fabrication practices.

The preference for Alloy 316/316L in cryogenic applications stems from various factors. Its low-temperature strength, overall corrosion resistance, excellent weldability, and low carbon composition make it an ideal material for the construction of cryogenic systems. Additionally, the alloy exhibits stable performance across a wide temperature range, facilitating its reliable and durable use in cryogenic environments. These features, especially the resistance to corrosion induced by liquid gases or chemical substances at low temperatures, contribute to its high performance and reliability in applications exposed to low temperatures [31].

Table 3.8 The Composition of 304L, 316L, 317L, and 2205 Steels.

Grade	UNS Number	Cr	Ni	Mo	N
304 L	S30403	18.2	8.1	0.1	0.06
316 L	S31603	16.2	10.2	2.2	0.06
317 L	S31703	18.2	11.2	3.2	0.06
S32003	S32003	21.5	3.7	1.8	0.17
2205	S32205	22.5	5.8	3.3	0.16

Table 3.9 Mechanical properties of 304L, 316L, 317L, and 2205 Steels.

Alloy	Yield Strength (MPa)	Tensile Strength (MPa)	Percent Elongation
304L	207	586	60
316L	303	607	57
317L	317	607	50
S32003	517	724	40
2205	586	862	30

Table 3.10 Thermal Conductivities and Thermal Diffusivities of Stainless Steels [32].

Thermal Properties	Metric
Specific Heat Capacity	0.500 J/g-°C @Temperature 0.000 - 100 °C
Thermal Conductivity	14.0 - 15.9 W/m-K
Melting Point	1375 - 1400 °C
Solidus	1375 °C
Liquidus	1400 °C
Maximum Service Temperature, Air	870 °C
	925 °C

3.1.6.2 Polymethyl Methacrylate

Plexiglass, a transparent thermoplastic material, is derived from polymethyl methacrylate (PMMA). The history of this material traces back to the early 20th century when German chemist Otto Röhm successfully synthesized a monomer called methyl methacrylate. Röhm aimed to create a transparent plastic material using this monomer.

In 1928, Otto Röhm achieved the polymerization of methyl methacrylate, resulting in a transparent plastic material. This material garnered attention for its durability, transparency, and lightweight properties. Röhm and his partner Otto Haas decided to market this new material under the name Plexiglas. In 1933, Rohm and Haas Company commercially introduced Plexiglas to the market.

Initially designed for military applications, Plexiglas found its place during World War II in products such as airplane windows, canopies, and turrets. Post-war, Plexiglas gained popularity in civilian applications, being utilized in various industries such as retail displays, signs, lighting fixtures, and furniture.

Today, Plexiglas is a versatile material available in different colors, thicknesses, and styles, serving as a preferred choice in many industrial and design applications. The success story of Plexiglas illustrates its significant role in materials science and industrial applications.

Plexiglas material has been chosen for the application of a cooling chamber to prevent thermal bridging between the inner and outer shells. As seen in Table 5, Plexsiglass exhibits a very low thermal conductivity coefficient alongside a relatively high tensile strength. Its widespread preference in industrial applications ensures easy availability [33].

Table 3.11 Overview of Materials for Acrylic [34].

Physical Properties	Metric
Density	1.18 - 1.19 g/cc
Water Absorption	0.130 - 0.800 %
Water Absorption at Saturation	0.650 - 2.60 %
Moisture Expansion	0.500 %
Moisture Vapor Transmission	55.0 cc-mm/m²-24hr-atm

Mechanical Properties	Metric
Hardness, Barcol	49.0 - 50.0
Hardness, Rockwell M	94.0 - 105
Ball Indentation Hardness	175 MPa
Tensile Strength, Ultimate	62.0 - 83.0 MPa
	40.0 - 110 MPa @Temperature -40.0 - 70.0 °C
Tensile Strength, Yield	64.8 - 83.4 MPa
Elongation at Break	3.00 - 6.40 %
Modulus of Elasticity	2.76 - 3.30 GPa
Flexural Yield Strength	98.0 - 125 MPa
Flexural Modulus	2.96 - 3.30 GPa
Compressive Yield Strength	110 - 124 MPa
Compressive Modulus	2.76 - 3.03 GPa
Poissons Ratio	0.370
Shear Modulus	1.70 GPa
Shear Strength	25.5 - 62.1 MPa
Izod Impact, Notched	0.160 - 0.220 J/cm
Izod Impact, Notched (ISO)	1.60 kJ/m²
Charpy Impact Unnotched	1.20 - 2.17 J/cm²
Coefficient of Friction	0.450 - 0.800
Compression Set	0.750 %

Thermal Properties	Metric
CTE, linear	39.0 - 198 µm/m-°C
Specific Heat Capacity	1.46 - 2.16 J/g-°C
Thermal Conductivity	0.187 - 0.209 W/m-K
Maximum Service Temperature, Air	70.0 - 200 °C
Deflection Temperature at 0.46 MPa (66 psi)	110 - 225 °C
Deflection Temperature at 1.8 MPa (264 psi)	86.0 - 215 °C
Vicat Softening Point	105 - 118 °C
Minimum Service Temperature, Air	-40.0 - -32.2 °C
Flammability, UL94	HB
Flame Spread	5.84 - 36.0 mm/min
Flash Point	425 - 488 °C
Smoke Density	5.00 - 65.0

3.1.6.3 S235 JR Galvanized Steel

S235JR steel has been widely utilized in structural steel applications. This material class is generally based on the EN 10025-2 standard and possesses specific mechanical and chemical properties.

Galvanized steel, on the other hand, refers to steel products processed with a zinc coating. The zinc coating is applied to protect the steel against corrosion, enhance durability, and provide an aesthetic appearance.

S235JR galvanized steel represents a form of S235JR steel class processed with a zinc coating. This process can enhance the steel's resilience against external factors and elevate its resistance to corrosion. Additionally, it has been preferred in various application areas by improving the aesthetic appearance of the steel material.

Galvanized steel has found widespread use in the construction sector, roof coverings, railings, the automotive industry, and outdoor applications. The zinc coating serves to protect the steel against various atmospheric conditions, making it a long-lasting and durable material [35].

Table 3.12 Material Properties of Steel [36].

Tensile Strength, Yield	>= 185 MPa @Thickness 150.1 - 200 mm
	>= 195 MPa @Thickness 100.1 - 150 mm
	>= 215 MPa @Thickness 40.1 - 63.0 mm
	>= 215 MPa @Thickness 63.1 - 100 mm
	>= 225 MPa @Thickness 16.1 - 40.0 mm
	>= 235 MPa @Thickness <=16.0 mm
Elongation at Break	21 % @Thickness 150.1 - 200 mm
	22 % @Thickness 100.1 - 150 mm
	24 % @Thickness 63.1 - 100 mm
	25 % @Thickness 40.1 - 63.0 mm
	26 % @Thickness <=16.0 mm
	26 % @Thickness 16.1 - 40.0 mm
Modulus of Elasticity	210 GPa
Poissons Ratio	0.30
Shear Modulus	80.0 GPa

Thermal Properties	Metric
CTE, linear	12.0 µm/m-°C @Temperature 20.0 - 300 °C
Specific Heat Capacity	0.460 - 0.480 J/g-°C @Temperature 50.0 - 100 °C
Thermal Conductivity	40.0 - 45.0 W/m-K
Transformation Temperature	485 °C
	725 °C
	863 °C

3.1.7 Structural Design Analysis of the Cabin

The Ansys Workbench 2021 program was utilized for structural analysis. The analysis type is limited to static analysis only because there is no impact of shock or vibration on the structure. Since the structure is generally stable, static analysis is sufficient for the cabins to support each other. In this context, sheet metal parts and plexiglass parts will be analyzed separately. The yield stresses for these materials are provided in the sections related to structural materials. In this study thermal structural effects are neglected and all boundary conditions are applied at room temperature.

3.1.8 Structural Design Analysis of the Chamber 1

The structure under analysis has a very large geometry. Therefore, certain simplifications were made before starting the analysis. Radius and fillets have been removed to facilitate meshing. Since the structure is predominantly made of sheet metal, it has been converted into a shell model to reduce the solution time. The shell model for Chamber 1 is illustrated in Figure 3.28. Subsequently, it was loaded into the Ansys Workbench, where the static analysis module was added, as shown in Figure 3.29.

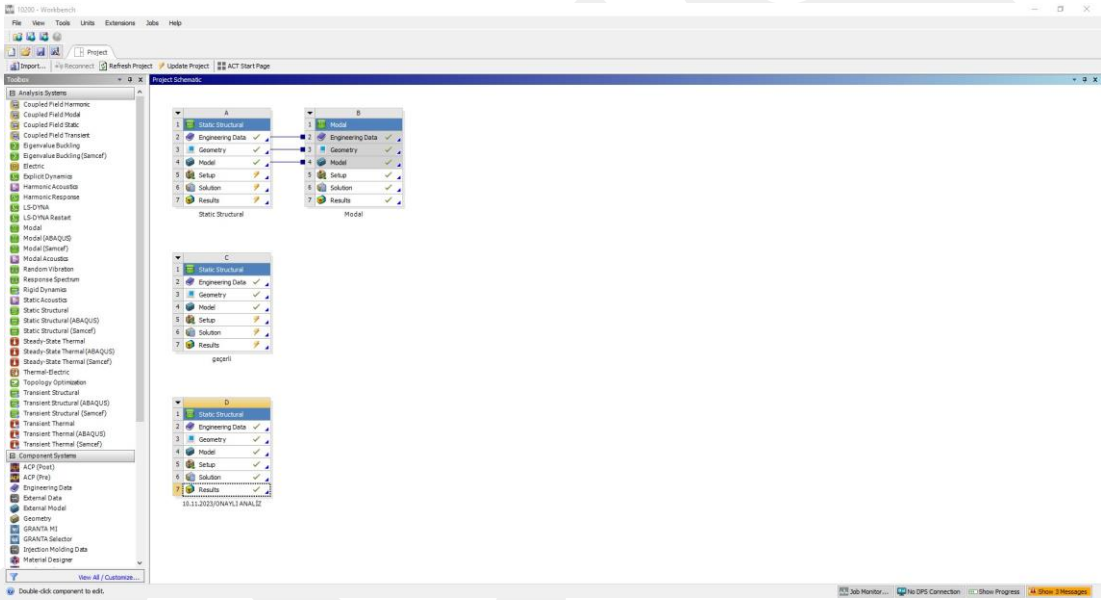

Figure 3.8 Workbench Static Structural Module.

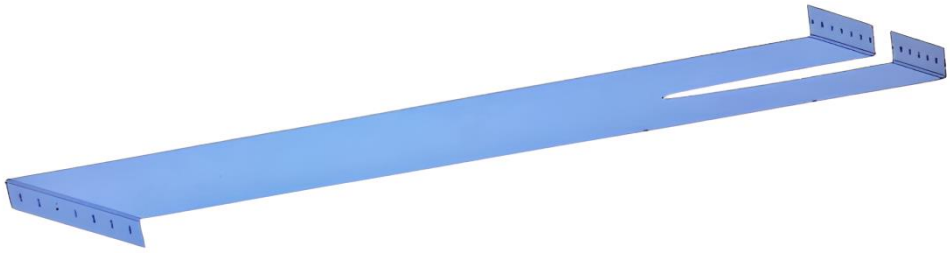

Figure 3.9 Shell Model of Part.

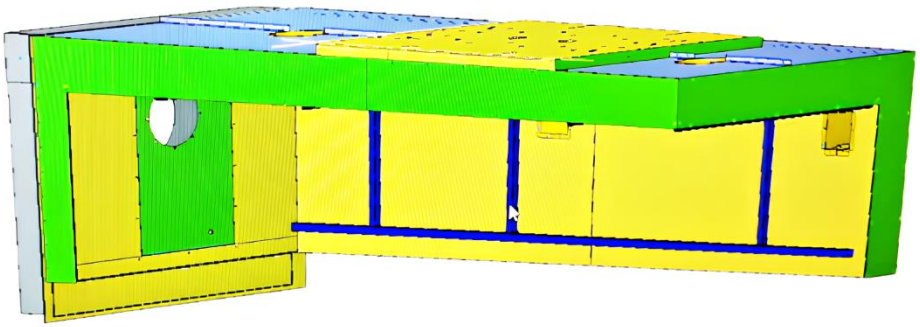

Figure 3.10 Shell Model of Chamber 1.

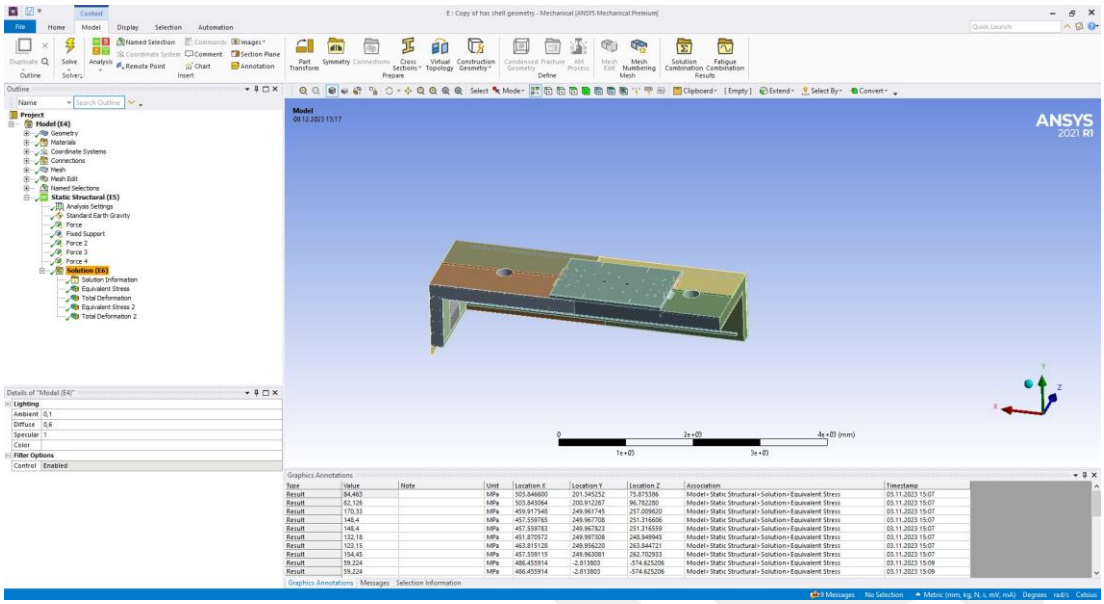

Figure 3.11 Chamber 1 in Workbench Window.

Bounding Box	
Properties	
Volume	1,0868e+008 mm³
Mass	516,76 kg
Scale Factor Value	1,
2D Tolerance	Default (1,e-005)
Statistics	
Bodies	87
Active Bodies	87
Nodes	910226
Elements	704515
Mesh Metric	Orthogonal Quality
Min	4,3324470907069E-04
Max	1
Average	0,993337712563675
Standard Deviation	0,041221280777895

Figure 3.12 Detail of Geometry.

3.1.9 Material Assigments

Once the analysis model is loaded, material assignments have been made individually to all components. The relevant materials were previously defined in the Workbench library and consist of three types used in the project.

Figure 3.13 Material Assignments.

3.1.10 Connections Algorithm

All bolts have been removed from the analysis model. Bolts are modeled using the beam elements, simplifying the geometry and reducing solution time. All nut-bolt and rivet connections are modeled as beam elements. To observe inter-surface sheer stresses on all bolt-nut connection surfaces modeled with beams, 'no separation contact' has been specified. Welded components are modeled as bonded, utilizing edge-to-edge contact. For the solution of welded surfaces, MPC (Multipoint Constraint) formulation has also been employed.

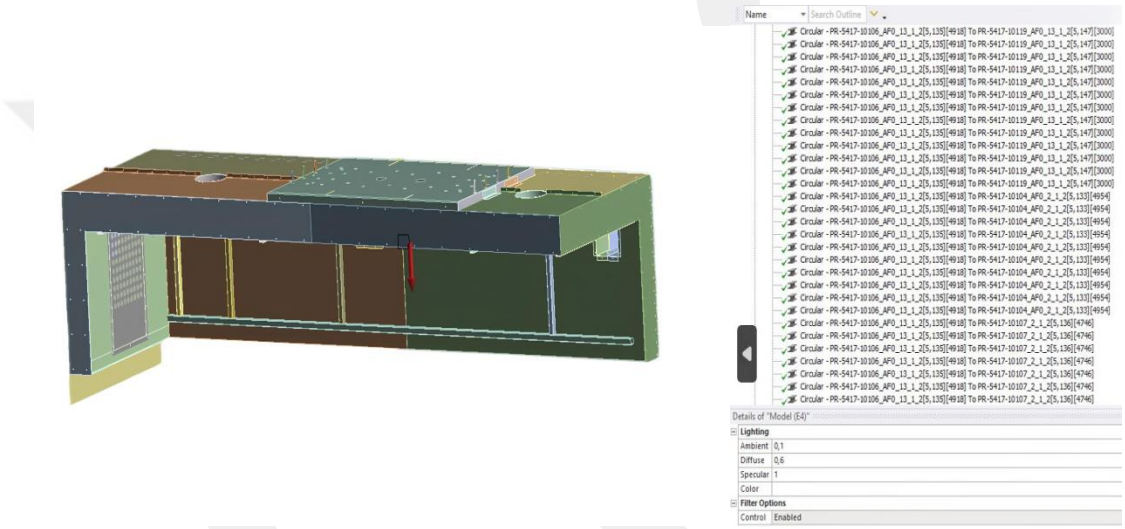

Figure 3.14 Beam Element Details.

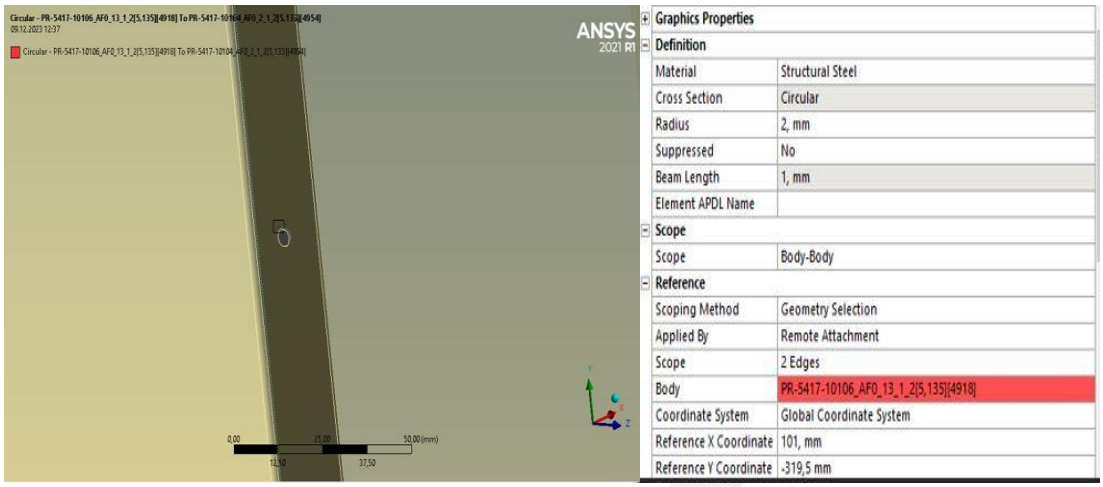

Figure 3.15 Beam Element Details-2.

3.1.11 Meshing Bodys And Mesh Metrics

Mesh quality is a critical factor influencing the accuracy and efficiency of simulations. Various criteria are employed to evaluate mesh quality, including element type, aspect ratio, jacobian determinant, area, minimum and maximum angles, skewness, and closeness to equilateral. Element types, such as triangles and quadrilaterals, need to be selected based on their suitability for different simulation types and compliance with analysis requirements. The aspect ratio, representing the ratio between element height and width, plays a crucial role, with closer aspect ratios being favorable for better mesh quality [37]. The Jacobian determinant, indicating the deformation during the transformation of elements from local to global coordinate systems, needs to be positive and large for desirable mesh quality. Additionally, considerations such as area, angles, skewness, and equilateral characteristics contribute to the overall assessment of mesh quality. Ultimately, good mesh quality is paramount for achieving accurate and reliable simulation results [38].

3.1.12 Skewness Ratio

Skewness Ratio" is a parameter that measures the irregularity of corners in an element. This ratio helps determine how skewed or irregular the geometric shape of an element is.

Skewness is typically defined as the lack of symmetry between the edges or corners of an element. In an ideal scenario, the corners of an element should be placed in a regular manner, and the skewness ratio should be low. High skewness ratios may indicate that the element has undergone unwanted deformation or is irregular.

Only for triangels and tetrahedrons equilateral elements skewness ratio described as

Equilateral Volume Deviation Skewness = $\frac{Optimal\ cell\ size - cell\ size}{Optimal\ cell\ size}$

Hexagonal, prsims and pyramids shape elements and all type of cell and face shapes

Normalized Angle Deviation Skewness= $\max[\frac{\theta_{max}-\theta_e}{180-\theta_e}, \frac{\theta_e-\theta_{min}}{\theta_e}]$ 

Tetrahedra and triangles have interior angles close to approximately 60 degrees, while quadrilaterals and hexahedra have interior angles close to approximately 90 degrees, representing surfaces/cells that are geometrically equiangular [39].

Skewness mesh metrics spectrum

Excellent	Very good	Good	Acceptable	Bad	Unacceptable
0-0.25	0.25-0.50	0.50-0.80	0.80-0.94	0.95-0.97	0.98-1.00

Figure 3.16 Skewness Ratio Quality Chart.

3.1.13 Orthogonal Quality

Orthogonal Quality refers to a measure of how close the elements in a mesh are to being perfectly orthogonal or perpendicular to each other. This metric is particularly relevant in finite element analysis (FEA) simulations, where having elements that are as orthogonal as possible is often desirable for accurate and reliable results.

The Orthogonal Quality value is a measure of the deviation from orthogonality, and a higher value indicates a larger deviation. Ideally, the Orthogonal Quality value should be as close to 1.0 as possible, representing perfectly orthogonal elements [40].

3.1.14 Aspect Ratio

Aspect Ratio refers to a measure of the geometric quality of elements in a mesh. Specifically, it assesses how elongated or distorted the elements are. The aspect ratio is calculated by comparing the length of the longest side to the length of the shortest side of an element. A low aspect ratio value indicates that the element is more equilateral or close to a regular shape, while a high aspect ratio value suggests that the element is more distorted or elongated. An aspect ratio value close to 1 indicates that the elements are more geometrically balanced and less elongated or distorted. This situation signifies good mesh quality. Smaller aspect ratio values are generally associated with better mesh quality because the elements resemble squares more closely, which often helps in achieving more accurate and reliable results [41].

3.1.15 Defination of Boundry Conditions

The design includes two different chambers. These chambers have distinct boundary conditions among themselves; therefore, the definitions have been separately established within their respective contexts.

3.1.16 Chamber 1 Boundry Conditions

According to the assembly details of Chamber 1, eight bolts of size M16, as shown in Figure 12, will be connected to the steel construction interface at the upper region. Meanwhile, Chamber 2 will be mounted on a transport trolley and will not be under any load. However, after the conditioning process, Chamber 2 will be detached from the upper chamber for lifespan tests. During this period, the upper chamber will carry its own weight. Therefore, the ends of these bolts have been defined as fixed support. Gravity force has been applied in the -y direction. Additionally, during the connection of the chamber to the interface, reaction forces will be generated. Hence reaction forces from these surfaces have been applied.

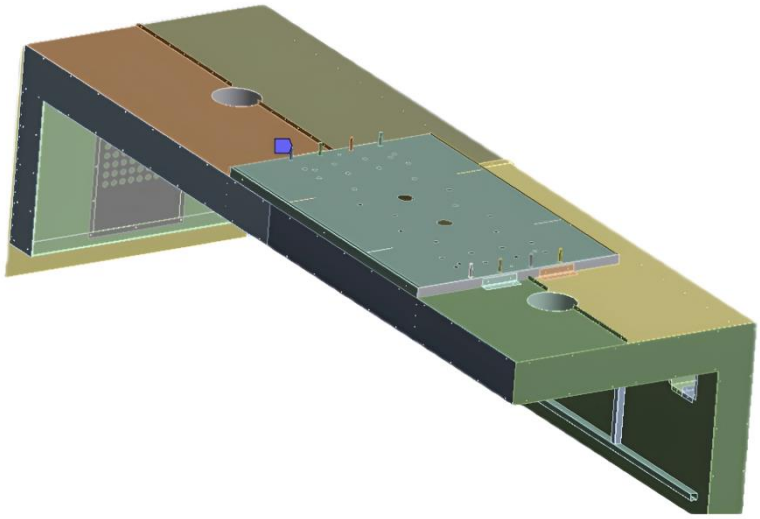

Figure 3.17 Fixed Support Bolt of Chamber 1.

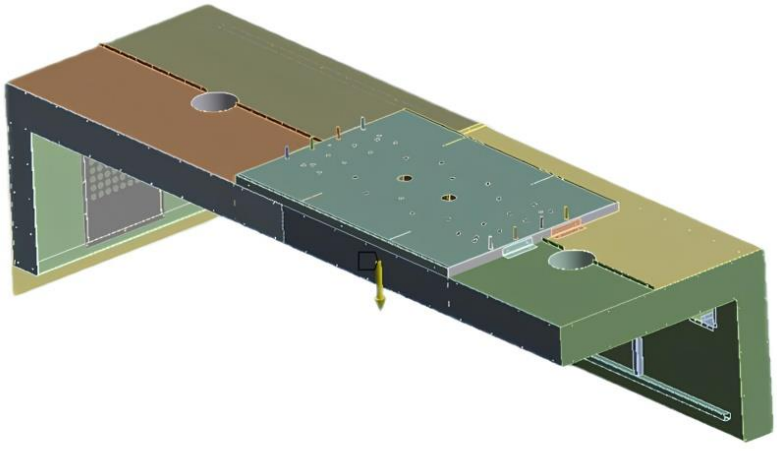

Figure 3.18 Earth Gravity of Chamber 1.

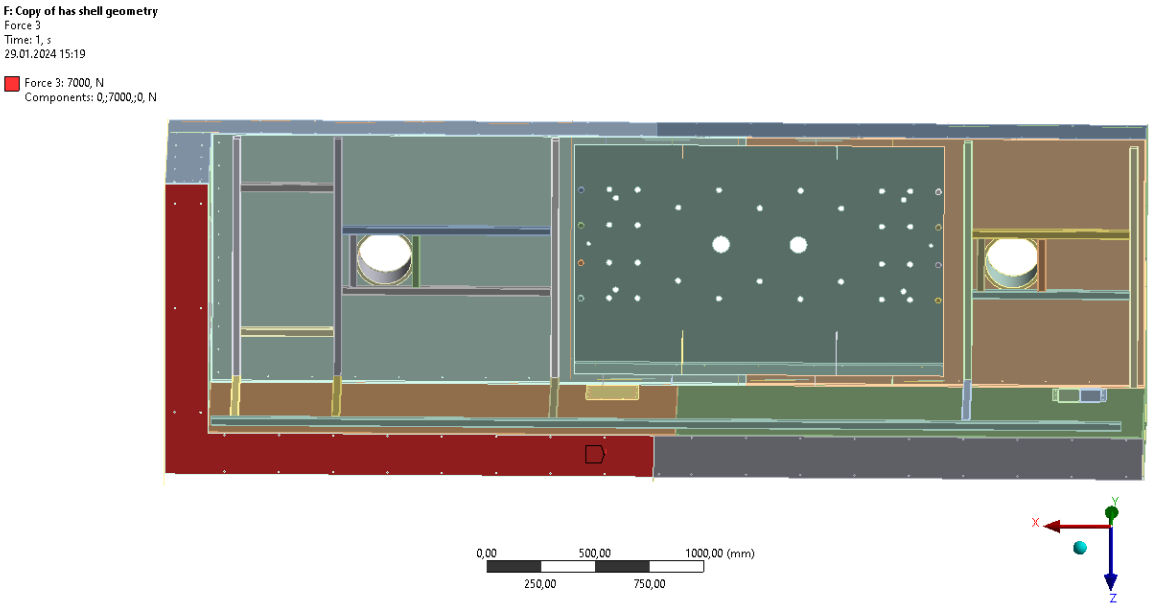

Figure 3.19 Mass of The Chamber 2 is Reaction Forces of Chamber 1 Lifting Surfaces.

3.1.17 Chamber 2 Boundry Conditions

Chamber 2 is mounted on the transport trolley with its bottom surface fixed. Therefore, the entire bottom base has been defined as a fixed support. In addition, when loaded onto the transport trolley, the weight of Chamber 1 also acts as a force on the contact surfaces of Chamber 2. Considering safety factors, these forces have been defined and applied to the relevant contact surfaces as a surface region.

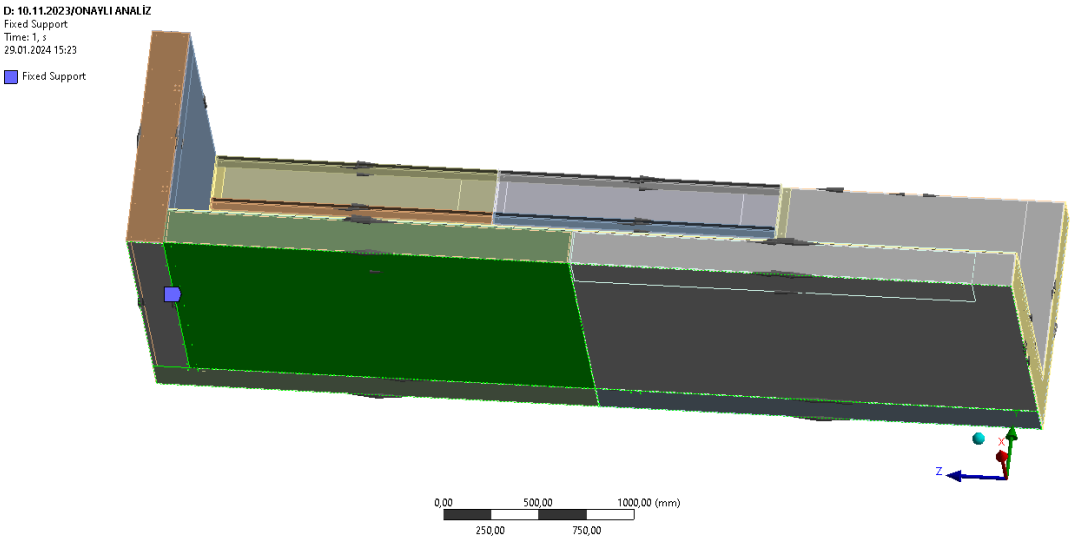

Figure 3.20 Bottom Surface is Fixed Support of Chamber 2.

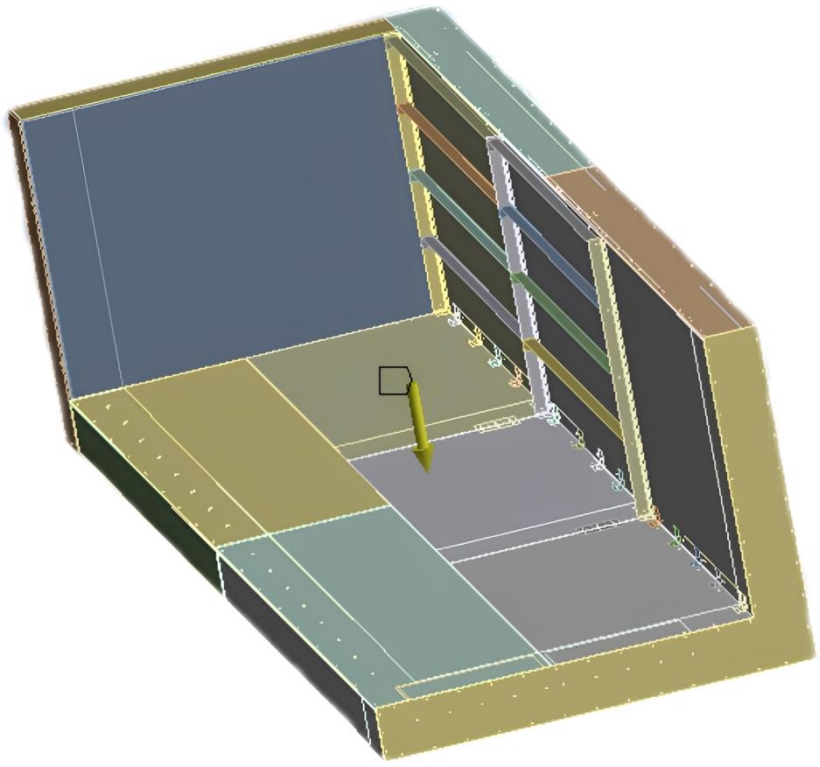

Figure 3.21 Earth Gravity of Chamber 2.

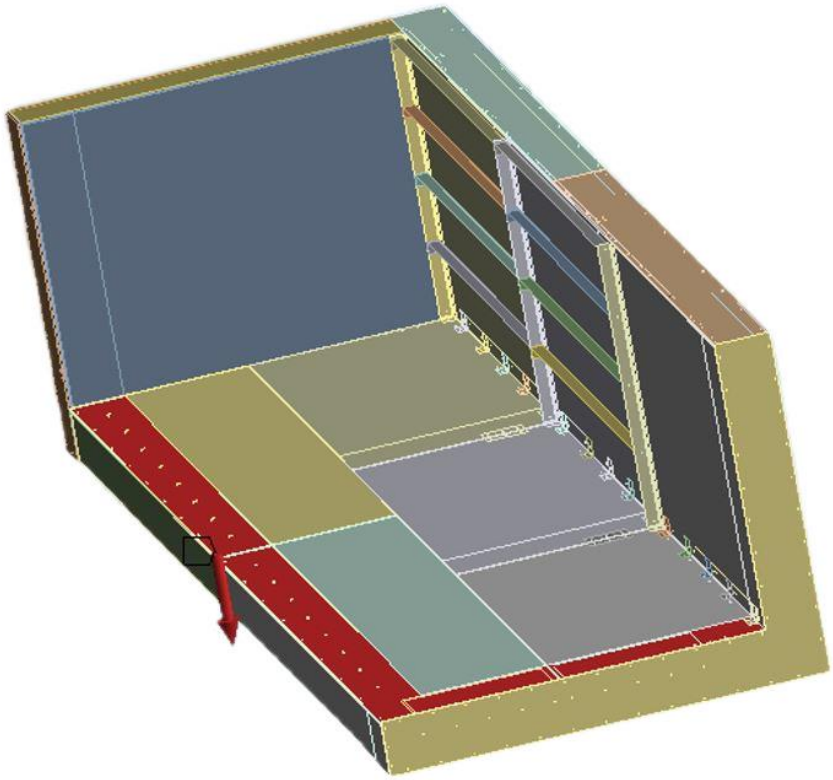

Figure 3.22 Mass of the Chamber 1 is Reaction Forces of Chamber 2 Lifting Surfaces.

CHAPTER 4

RESULTS AND DISCUSSION

In this chapter, the results will be examined, verified, and interpreted.

4.1 Coolant Types and Calculation Equations for Determining the Required Coolant Amount

The cooling process within the cabin is achieved through the supply of cryogenic liquid without employing any refrigeration cycle. The first step in this process is deciding on the type of cryogenic liquid. Considering that the test chamber will be cooled to -55°C, cryogenic liquids with an evaporation temperature below -55°C were examined. As indicated in Table 3.2, which outlines the characteristics of liquids used in cryogenic applications, all commonly used cryogenic liquids evaporate at temperatures significantly below -55°C. Therefore, this criterion could not be employed as a decisive factor.

Subsequently, the expansion coefficients of the cooling liquids were studied. Nitrogen gas, with a phase transition coefficient of 710 times, was selected due to its rapid expansion rate. One of the challenges encountered during the design phase is the potential for rapidly expanding cryogenic liquid to reach pressures well above atmospheric pressure, surpassing the structural strength values of the cooling chamber. In addition to the aforementioned parameters, the decision-making process for cryogenic liquid selection extended to a scrutiny of enthalpy and specific heat values. These crucial parameters are delineated in Table 3.2 for a comprehensive evaluation. Notably, at the standard boiling point, liquid oxygen exhibits the highest exothermic enthalpy at -4263 J/mol, followed closely by liquid nitrogen with the

second-highest exothermic enthalpy at -3401 J/mol. Subsequently, liquid neon claims the third position with an enthalpy of -1203 J/mol.

Comparing specific heat values, liquid nitrogen dominates with 57.79 J/mol·K at its boiling point, securing the top position, while liquid oxygen trails with a value of 52.22 J/mol·K. Neon follows closely as the third-highest enthalpy, registering 38.8 J/mol·K. Enthalpy is indicative of the total internal energy of the liquid, and as an exothermic reaction, a more negative enthalpy denotes a higher cooling internal energy. Additionally, a liquid with a high specific heat necessitates more heat during the vaporization process, thereby extracting more heat from the surroundings.

These properties not only play a pivotal role in the phase transition of the cryogenic liquid but also influence the cooling capacity during the subsequent transition to the gaseous phase. Consequently, alongside expansion coefficient considerations, these attributes emerge as critical criteria in the selection process. Upon meticulous examination of these characteristics, the decision converged on the selection of nitrogen gas. Additional to all technical spesification, this issue poses a challenge to be overcome in the design phase, nitrogen gas, with the lowest expansion coefficient, was preferred in the selection of the cooling equipment.

According to the equations modeled in Jacobs' 1963 study titled "Cryogenic Liquid Consumption: Limits and Estimation," the required refrigerant quantity for the system below has been calculated [42].

In this section, all calculations will utilize Equation 3.12 and Table 3.3.

In accordance with standard room conditions, the initial temperature of the equipment slated for cooling is set at 298.15 K, representing room temperature. The target temperature for cooling is specified as 218.15 K. Consequently, the ϭ_min values have been extracted from Table 4.13.

Table 4.13 Specific Liquid-Nitrogen Requirement.

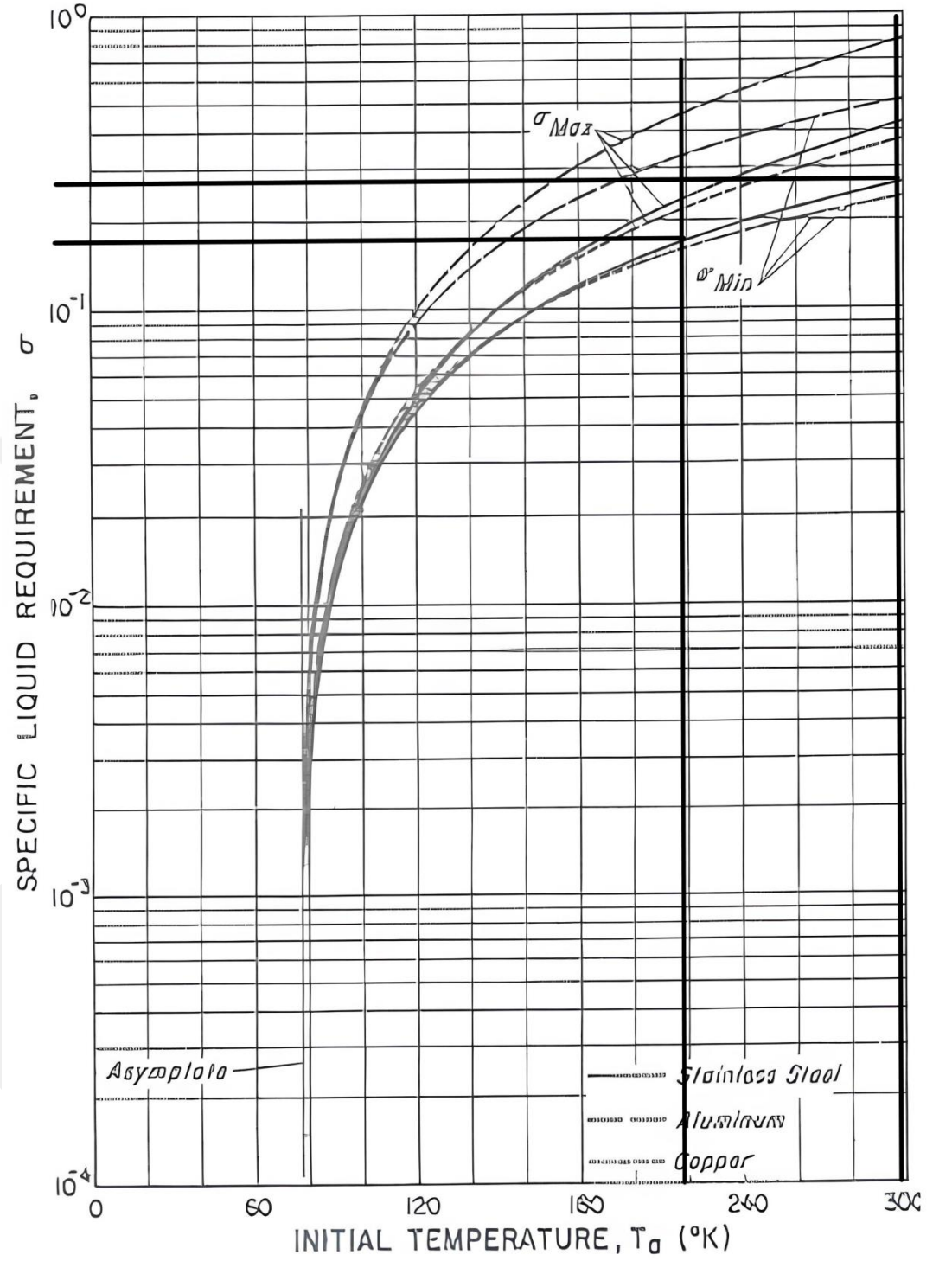

0,43-0,23=0,2*500=100kg

The chamber has 500 kg mass itself. 100 kg liquid nitrogen consumed for cooling only cabin structure.

4.2 Calculation of Cooling Existing Air in Chamber

The total interior volume of the cabin is calculated as 4600 mm in length, 1200 mm in width, and 800 mm in height, totaling 5 m^3.

According to the specified assumptions, the total air mass is calculated from the ideal gas equation in equation 3.13. Accordingly, there are 5.48 kg of air in this volume. The required mass of liquid nitrogen to cool this air is calculated using equation 3.14, based on the ideal gas equation and the law of conservation of energy. Room conditions were assumed in the previous section and are 25°C. Accordingly, the mass of nitrogen required to heat the air inside is 3 kg. The specific heat value for air is shown in table 3.4.

Table 4.14 Psychrometric Chart for 25°C and % 60 Humudity.

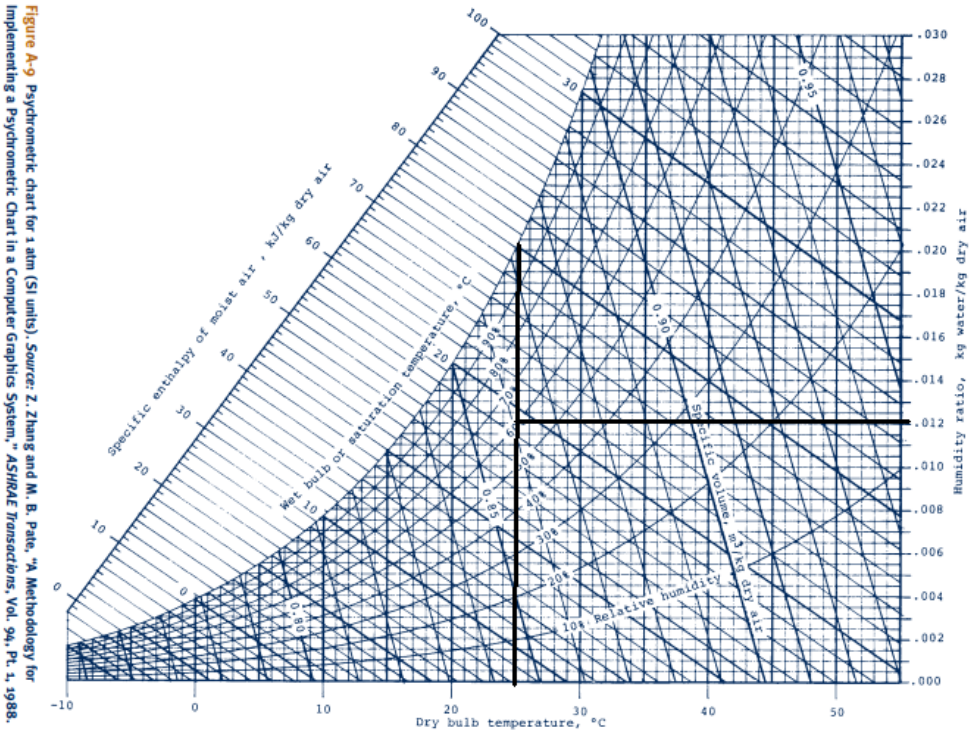

Figure A-9 Psychrometric chart for 1 atm (SI units). *Source:* Z. Zhang and M. B. Pate, "A Methodology for Implementing a Psychrometric Chart in a Computer Graphics System," *ASHRAE Transactions*, Vol. 94, Pt. 1, 1988.

In accordance with Ankara conditions, it is possible to use the value obtained from the psychrometric chart to calculate the humidity ratio in air conditions. According to the provided information, the value of grams of water vapor per kilogram of air is determined as 12 gram from pycometric chart in table 4.14. This value is commonly referred to as specific humidity and is typically expressed in units of grams of water vapor per kilogram of air. The total air mass was calculated as 5.48 kg in the previous section. According to this, considering that the cooling chamber is isolated and there is no air intake, the total frost formation amount is calculated as 65.76 grams [43].

The calculation for the total cooling load has been performed based on the useful load to be cooled and the amount of air inside the cooling chamber. According to these calculations, to cool the structure of the cabin and the air inside it, 103 kg of liquid nitrogen is required per test. Using Equation 12, it has been calculated that 200 kg of liquid nitrogen is needed to cool a payload of 1000 kg. Therefore, a tank

containing a total of 200 kg of liquid nitrogen can be used to test a payload of up to 1000 kg. Liquid nitrogen tanks designed for this requirement can supply the needed 200 kg of nitrogen with a standard 240-liter tank. Therefore, a 240-liter liquid nitrogen tank has been chosen.

Figure 4.23 240 Lt Nitrogen Liquid Tank [44].

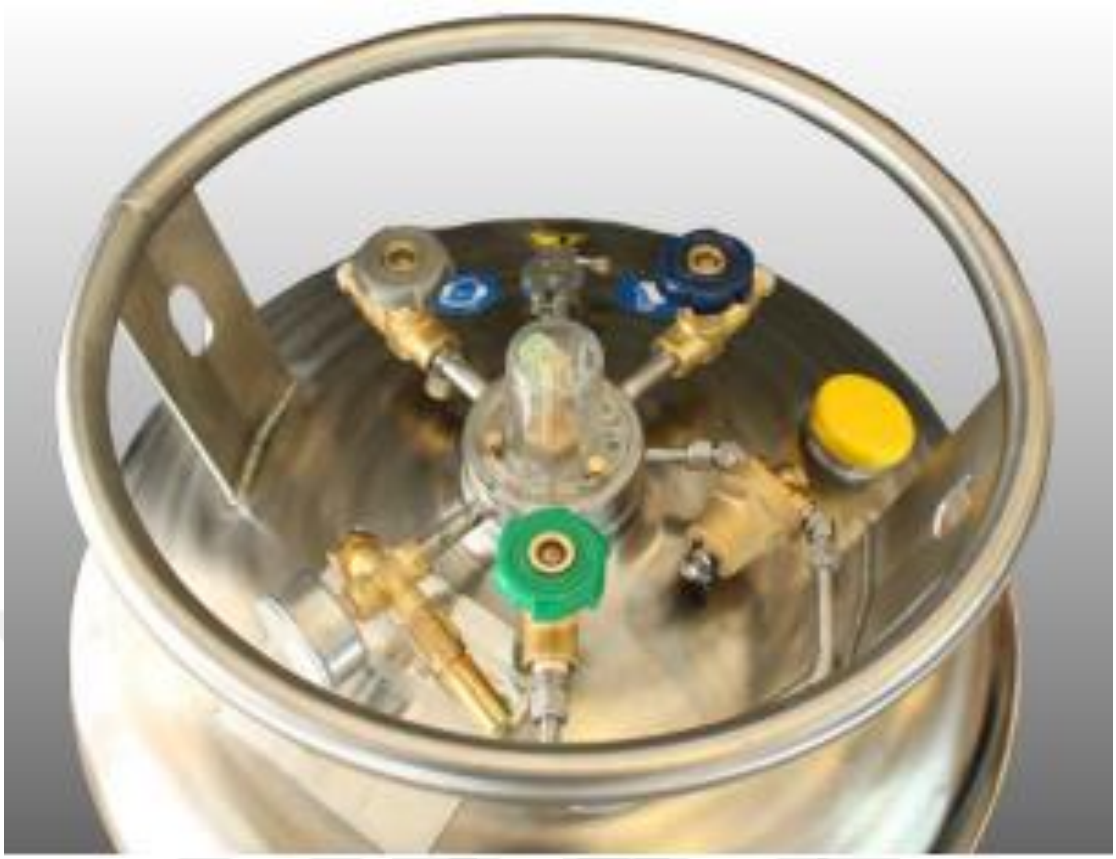

Figure 4.24 240 Lt Nitrogen Liquid Tank Piping [45].

4.3 Insulation Thickness Calculations and Material Selection

The insulation foam has been preferred due to its lightweight nature and lower thermal conductivity compared to other counterparts. Heat loss calculations have been made based on this choice.

The necessary insulation thickness has been calculated. The chosen insulation material is liquid-applied polyurethane foam, selected due to its thermal conductivity coefficient of approximately 0.002 W/mK. In addition to this foam, 1mm thick 316L and S235 JR sheet metal materials are incorporated into the inner and outer walls, with their respective thermal conductivity coefficients detailed in the material selection section.

The insulation thickness was then calculated for a thermal conductivity of 8 W/m, resulting in a thickness of 200 mm. The total heat loss was calculated as 147.2 W,

obtained by multiplying the heat flux by the total surface area of the walls causing heat loss.

$$\lambda_{insulatin} = 0{,}02\ \frac{W}{m\,K}$$

$$\lambda_{316L} = 16\ \frac{W}{m\,K}$$

$$\lambda_{S235JR} = 45\ \frac{W}{m\,K}$$

$$\sum \mathrm{R}_{TOTAL} = 10\ \frac{W}{m^2 K}$$

$$\varphi = 8\frac{W}{m^2}$$

$$\theta = 147{,}2\ W$$

4.4 Heating Capacity Calculations

The calculations have been performed with the previously calculated 5.67 kg of air. Enthalpies of the air at 1 atm pressure and at 25℃ and 70 ℃ have been read from thermodynamic tables 3.2 and substituted into the equation. The heating process can be carried out with a total of 226.2 kJ of energy. In the cooling calculation, as previously used, the weight of the cabin in direct contact with nitrogen is about 500 kg. There is a requirement for the useful load to be 1000 kg. Therefore, the total mass is assumed to be 1500 kg. In the next section, the specific heat value for AISI 316L is read from the material properties table, and calculations are performed by substituting it into equation 3-2. 33,750 kJ of heat energy is sufficient to carry out the required conditioning. As mentioned before, the value of 226.2 kJ required to heat the air remains very small compared to this result. The total heating requirement is 33,976.2 kJ. Since the heating process needs to be completed in 30 minutes or less, the required total power should be around 19 kW. Therefore, a selection of 12 electric resistors with a power of 2 kW each has been made and added to the design.

$$\emptyset = 5{,}67(340 - 300)$$

$$\Delta\emptyset \approx 226.2\text{kJ}$$

The specific heat capacity value for 316 stainless steel is read as 0.5 $\frac{j}{g\,℃}$ from Table 3-10.

$$\emptyset = 1500\,x\,500\;\;x\,(70-25)$$

$$\emptyset = 33{,}750kj$$

$$\emptyset_{Total} = 33750kj + 226{,}2kj$$

$$\emptyset_{Total} = 33976{,}2\;kj$$

4.5 Structural Design Materials and Thickness

For areas in contact with nitrogen, the cabin is constructed with 1 mm 316 L stainless steel and 5mm and 9.5 mm Plexiglass. The external shell, devoid of liquid nitrogen contact, is fabricated from 1 mm S235 JR galvanized steel.

Figure 4.25 The Produced Plexiglass Materials.

4.6 Meshing Bodys And Mesh Metrics

The meshing process has been completed with an average element size of 7 mm selected. Meshing has been performed for both the lower and upper cabins. Upon completion of this process, the average number of elements is around 2,000,000 for chamber 2 and 700000 element for chamber 1. For the measurement of mesh quality, the values of 'aspect ratio,' 'skewness ratio,' 'orthogonal quality,' have been checked for both cabins.

Details of "Mesh"

Display	
Display Style	Use Geometry Setting
Defaults	
Sizing	
Quality	
Check Mesh Quality	Yes, Errors
Error Limits	Aggressive Mechanical
Target Quality	Default (0.050000)
Smoothing	Medium
Mesh Metric	Skewness
Min	1,3057e-010
Max	0,94661
Average	0,15529
Standard Deviation	0,12703
Inflation	
Batch Connections	
Advanced	
Number of CPUs for Parallel Part Meshing	Program Controlled

Figure 4.26 Skewness Ratio Chamber 1.

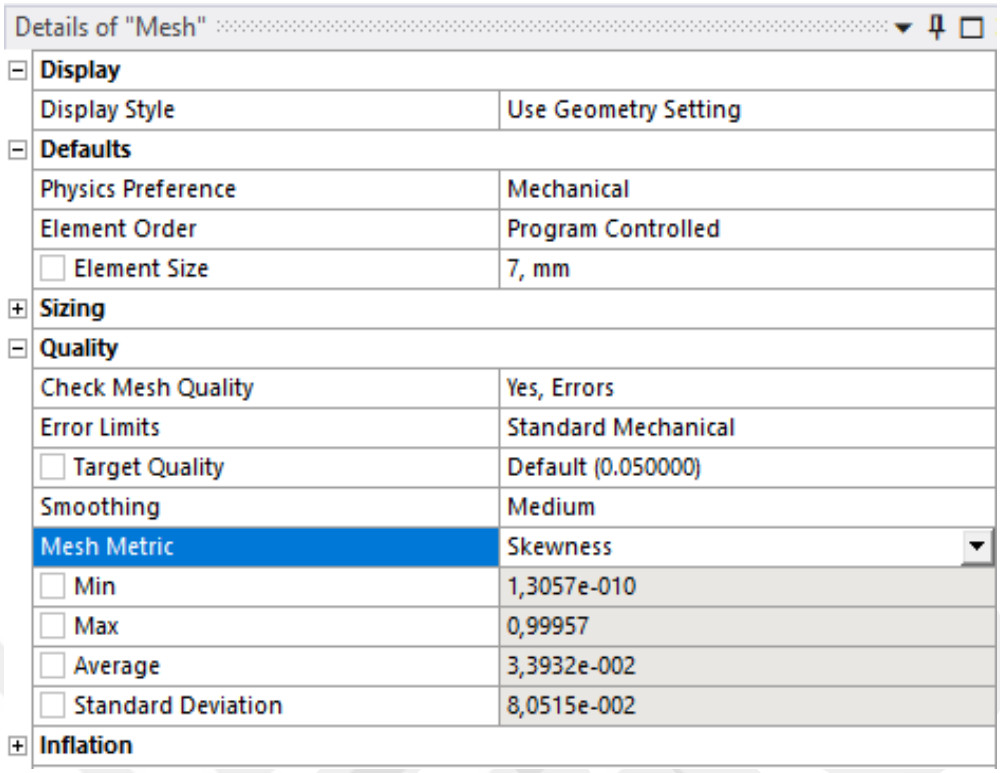

Details of "Mesh"

Display	
Display Style	Use Geometry Setting
Defaults	
Physics Preference	Mechanical
Element Order	Program Controlled
Element Size	7, mm
Sizing	
Quality	
Check Mesh Quality	Yes, Errors
Error Limits	Standard Mechanical
Target Quality	Default (0.050000)
Smoothing	Medium
Mesh Metric	Skewness
Min	1,3057e-010
Max	0,99957
Average	3,3932e-002
Standard Deviation	8,0515e-002
Inflation	

Figure 4.27 Skewness Ratio Chamber 2.

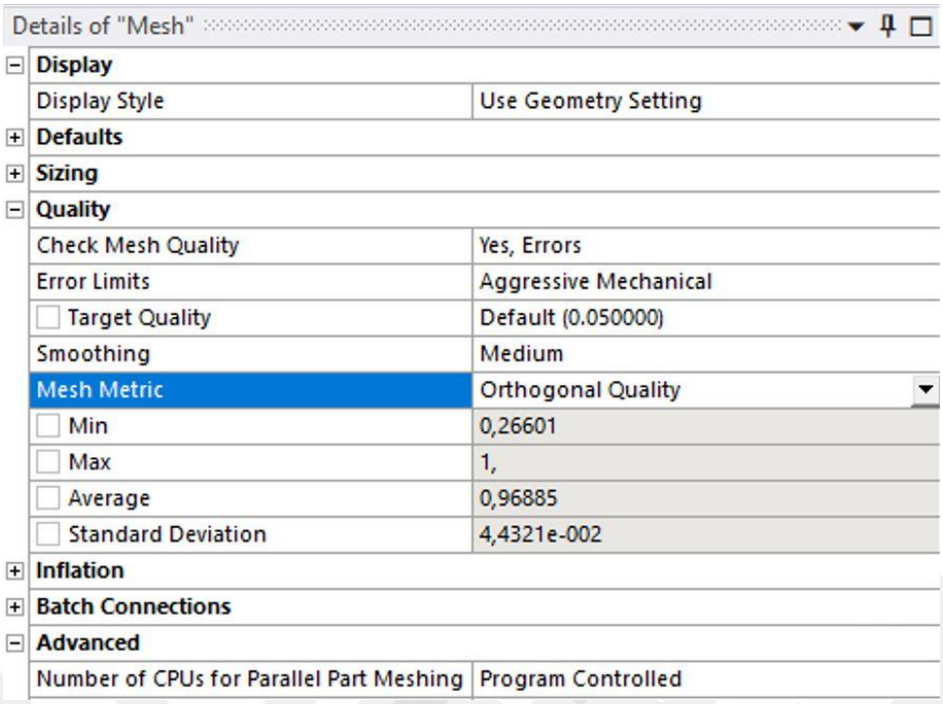

Figure 4.28 Orthogonal Quality Chamber 1.

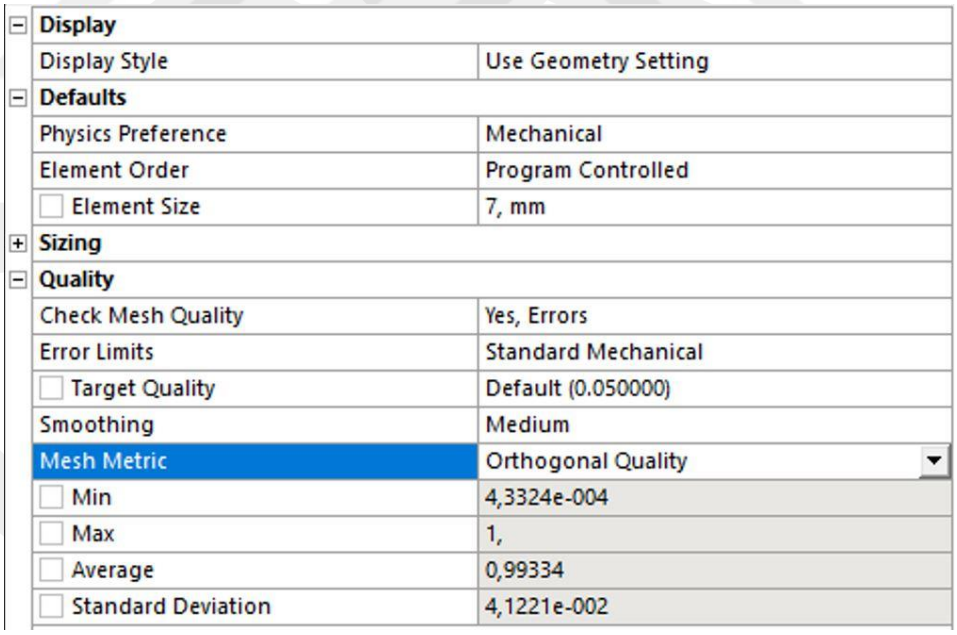

Figure 4.29 Orthogonal Quality Chamber 2.

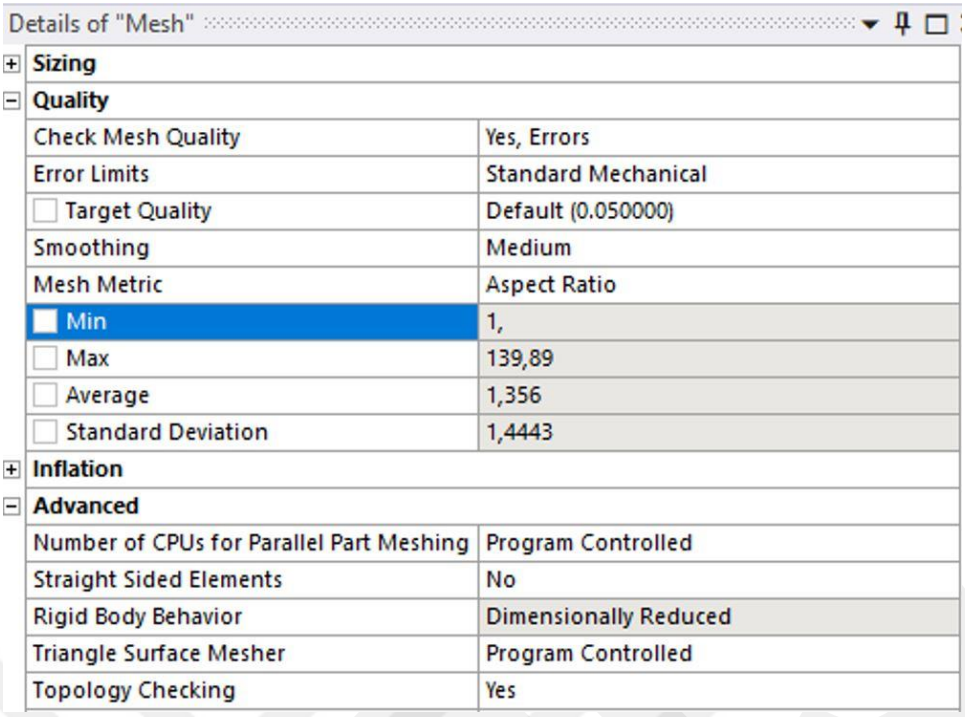

Details of "Mesh"

Sizing	
Quality	
Check Mesh Quality	Yes, Errors
Error Limits	Standard Mechanical
Target Quality	Default (0.050000)
Smoothing	Medium
Mesh Metric	Aspect Ratio
Min	1,
Max	139,89
Average	1,356
Standard Deviation	1,4443
Inflation	
Advanced	
Number of CPUs for Parallel Part Meshing	Program Controlled
Straight Sided Elements	No
Rigid Body Behavior	Dimensionally Reduced
Triangle Surface Mesher	Program Controlled
Topology Checking	Yes

Figure 4.30 Aspect Ratio Chamber 1.

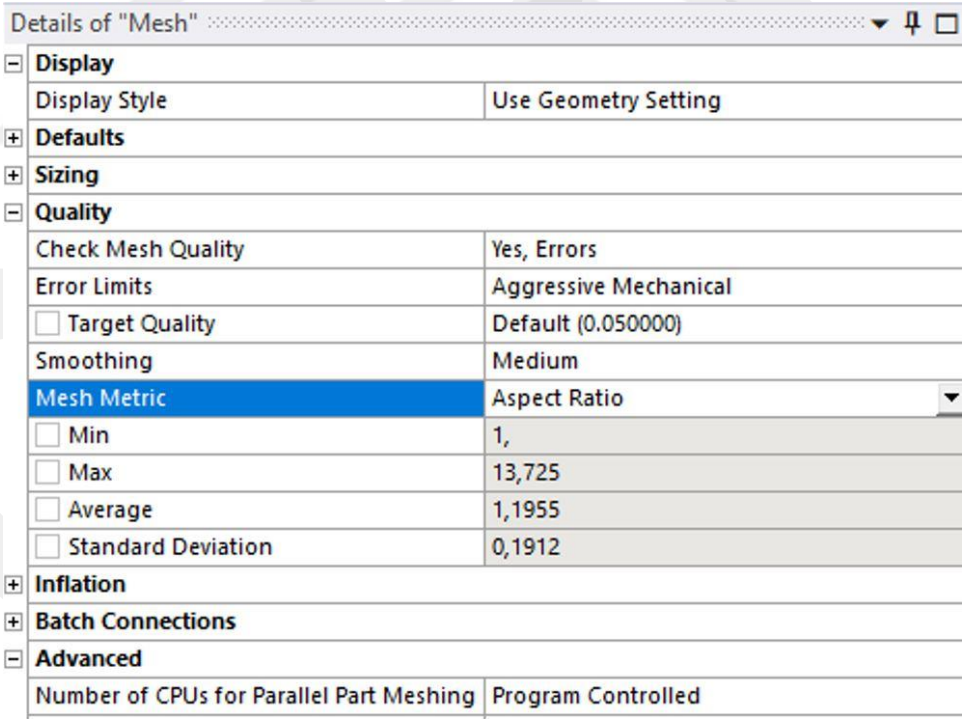

Details of "Mesh"

Display	
Display Style	Use Geometry Setting
Defaults	
Sizing	
Quality	
Check Mesh Quality	Yes, Errors
Error Limits	Aggressive Mechanical
Target Quality	Default (0.050000)
Smoothing	Medium
Mesh Metric	Aspect Ratio
Min	1,
Max	13,725
Average	1,1955
Standard Deviation	0,1912
Inflation	
Batch Connections	
Advanced	
Number of CPUs for Parallel Part Meshing	Program Controlled

Figure 4.31 Aspect Ratio Chamber 2.

Details of "Mesh"	
Display	
Display Style	Use Geometry Setting
Defaults	
Physics Preference	Mechanical
Element Order	Program Controlled
Element Size	7, mm
Sizing	
Quality	
Inflation	
Batch Connections	
Advanced	
Statistics	
Nodes	2228658
Elements	2218458

Figure 4.32 Mesh Statistic of Chamber 2.

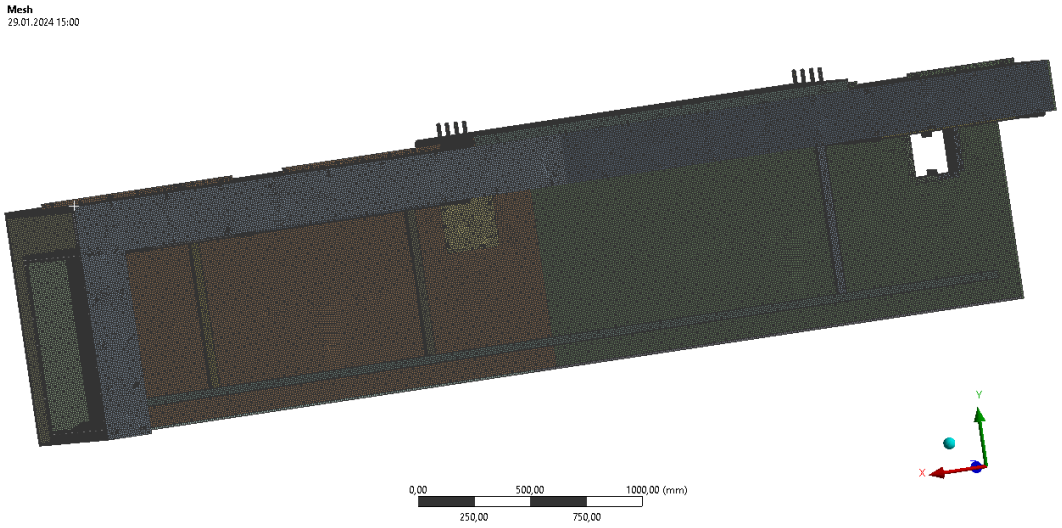

Figure 4.33 Chamber 1 –Meshing -1.

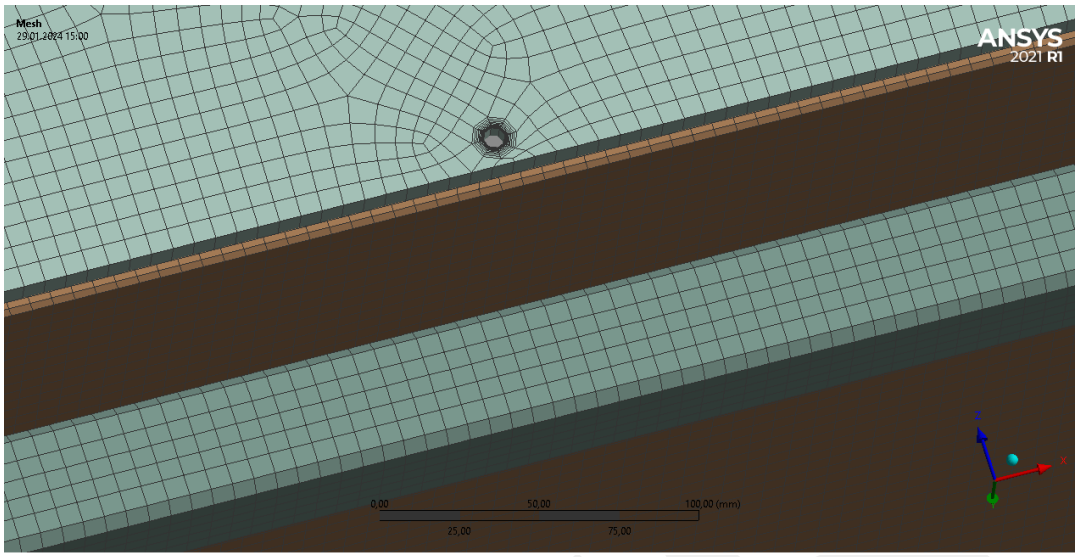

Figure 4.34 Chamber 1 –Meshing -2.

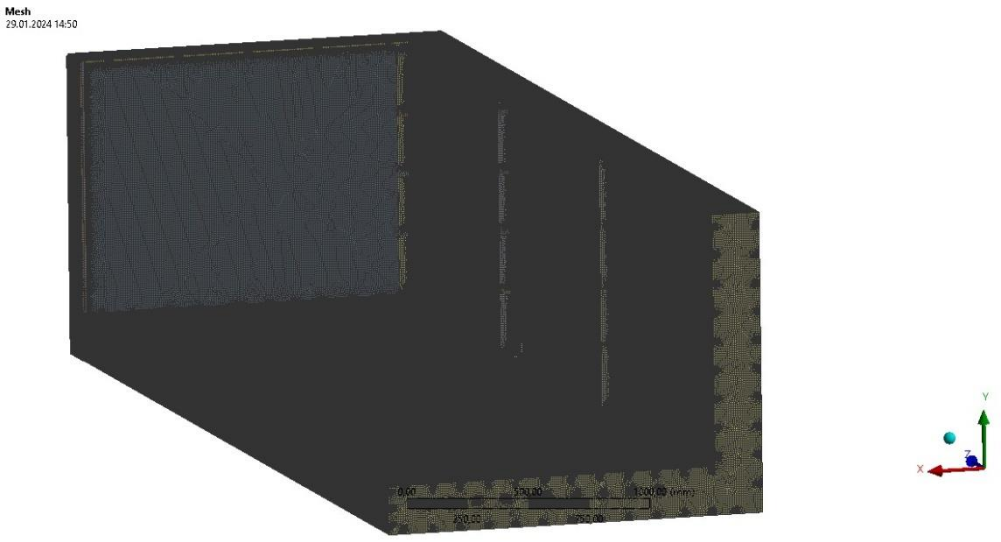

Figure 4.35 Chamber 2 –Meshing -1.

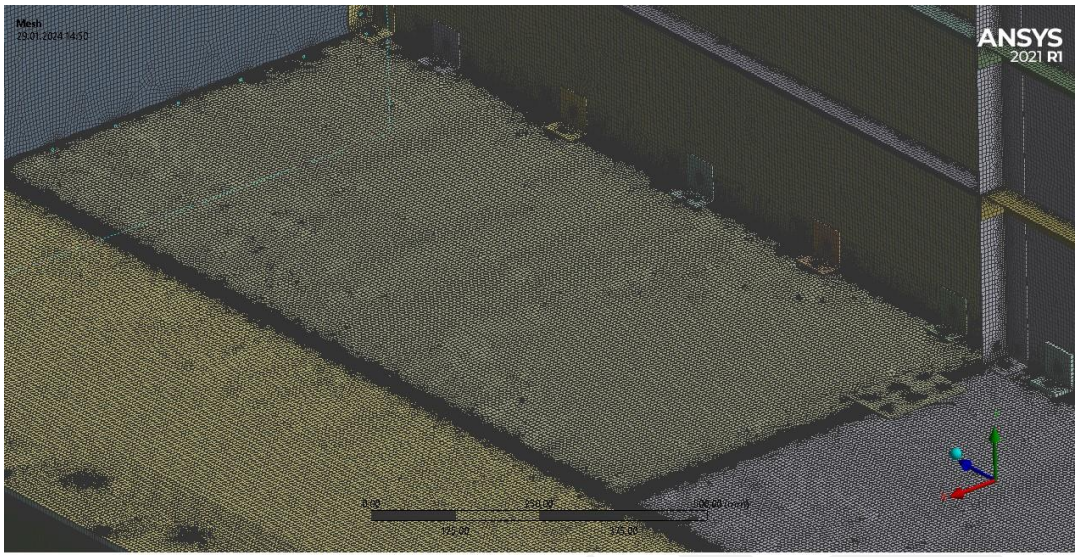

Figure 4.36 Chamber 2 –Meshing -2.

4.7 Structural Analysis Results

The results were examined based on the yield stresses of the materials. Generally, stresses remained within the safe range, except for some singular points. In Chamber 1, due to the direct loading on the Plexiglass material, loads on the material were analyzed separately. Despite the yield stress of the Plexiglass material being around 67 MPa, the loads on the material remained very low. Additionally, the M16 bolt connection was found to be suitable for the interface connection bolts in Chamber 1, and the loads around the bolts were observed to be within the safe range. No additional connection plates were required for load distribution.

For Chamber 2, design reinforcements were made and reanalyzed in areas where stresses were high on the contact surfaces of Chamber 1. The stresses on the reinforced contact surfaces were examined, and they were found to be within the safe range. Overall, the analysis results for Chamber 1 and Chamber 2 were reviewed, and it was observed that the existing design is safe after the reinforcements.

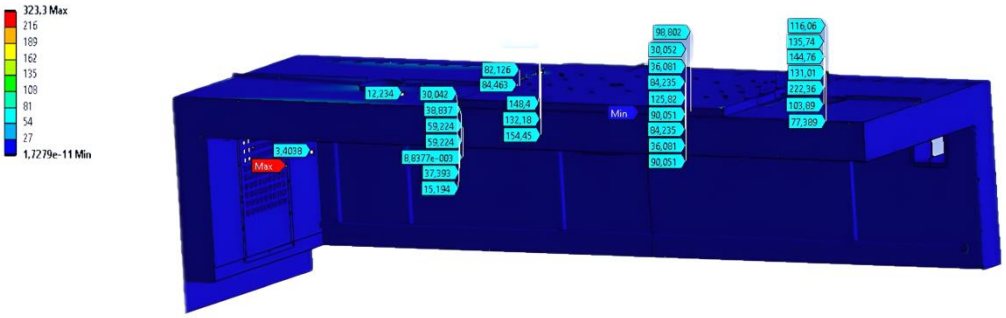

Figure 4.37 Chamber 1 Stress Results.

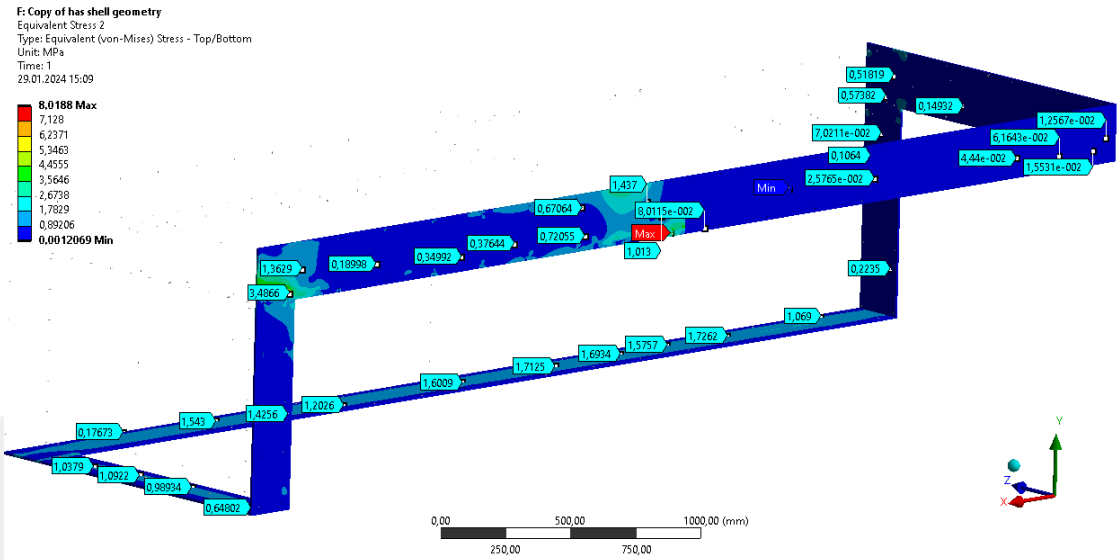

Figure 4.38 Chamber 1 Plexiglass Materials Stress Results.

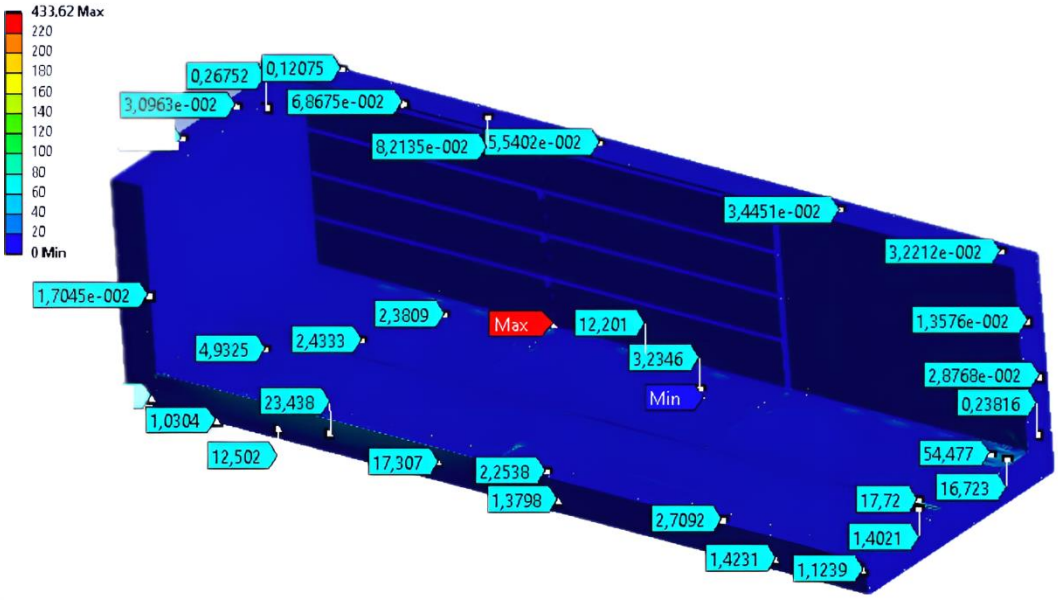

Figure 4.39 Chamber 2 Stress Results.

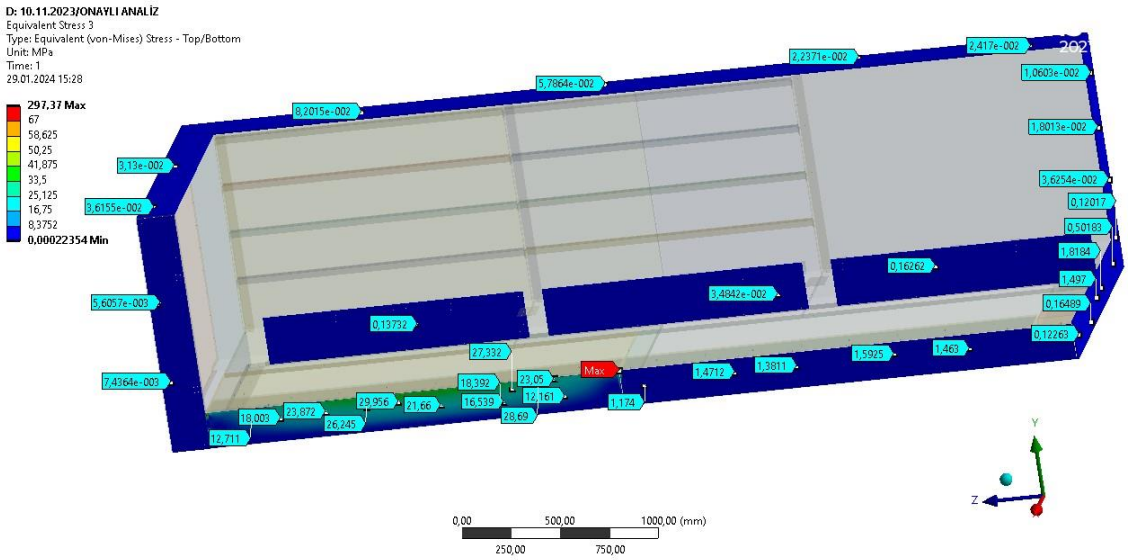

Figure 4.40 Chamber 2 Plexiglass Materials Stress Results.

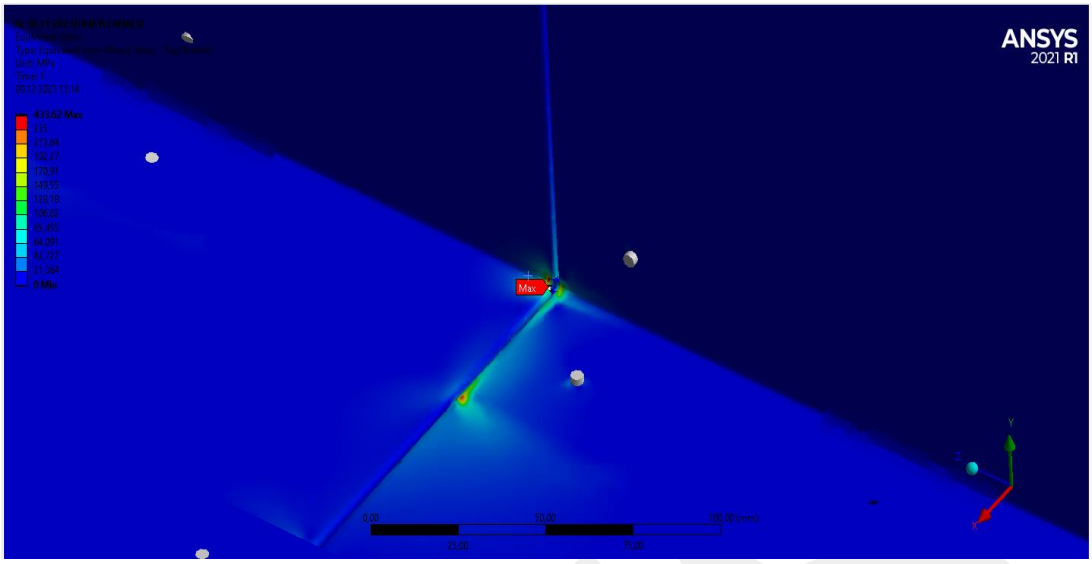

Figure 4.41 Chamber 2 Singularty Point.

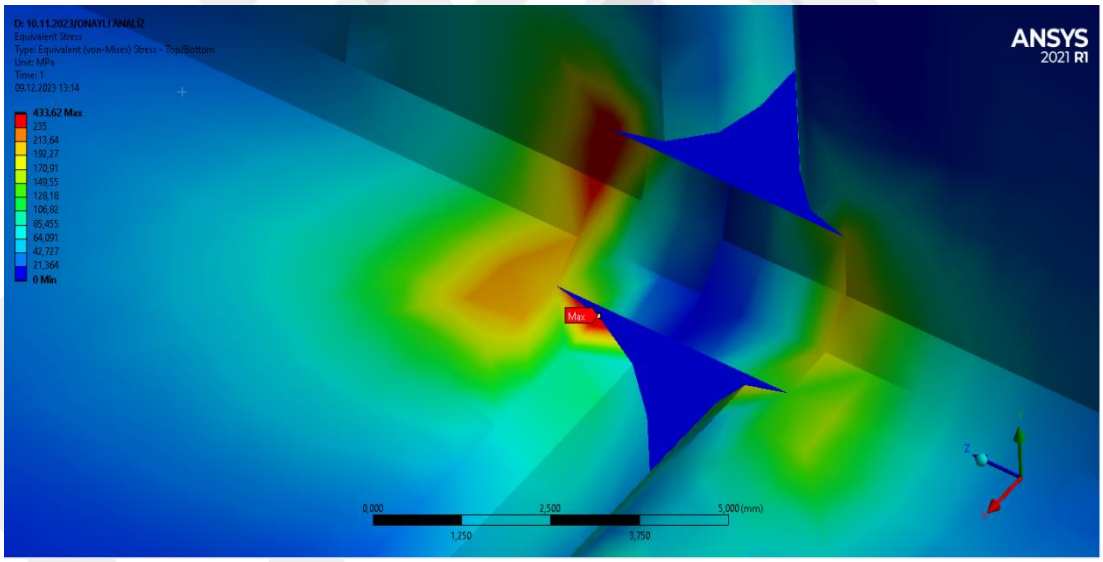

Figure 4.42 Singularty Points of Sheer Metali Rip Invervals.

During the design phase, when modeling sheet metal, rip intervals are defined at the corner pieces to prevent tearing during bending. These gaps are filled during production with welded manufacturing. In the design tool, filling these gaps requires the application of a welding module, where each gap must be filled individually.

When transitioning to the analysis model, potentially thousands of welds may need to be defined based on the design size. This not only imposes a significant computational burden on the processor but is also economically impractical in terms of labor. Therefore, these points with extreme stresses have been identified as singularity points during the analysis interpretation and have not been considered in the interpretation.

CHAPTER 5

CONCLUSIONS

In this thesis, a specialized conditioning chamber has been designed for the purpose of testing aviation and defense equipment. The geometry and operating conditions of the chamber were determined entirely based on the needs of the aviation and defense sectors. In the course of the study, the required amounts of cryogenic liquid for cooling processes, directly applied through liquid cryogenic fluids, were calculated. The continuous test quantity that can be performed in the chamber was determined based on the useful load. Material and equipment selection for the study were also addressed Additionally, the necessary insulation thicknesses for optimal heat loss were calculated.

Pre-manufacturing static analyses were conducted using Ansys Workbench software to anticipate and prevent potential deformations in the chambers. These analyses provided crucial insights into assessing the robustness and durability of the design. The study also emphasized potential future work on different applications of cryogenic liquids.

Recommendations:

1. Detailed studies on cooling and heating systems to optimize the design.
2. Evaluation of design improvements on transportation systems to enhance the chamber's portability.
3. Focus on future research on various applications of cryogenic liquids.
4. Comprehensive studies on the industrial-scale manufacturability and cost-effectiveness of the design.

5. These recommendations and findings can serve as a significant guide for the development, optimization, and successful real-world application of the design.

REFERENCES

[1] K. D. Timmerhaus and R. P. Reed, "Historical Summary of Cryogenic Activity Prior to 1950" in *Cryogenic Engineering.* 1st ed., vol. 2. R. Radebaugh, Ed. Boulder, CO 80309: Springer Science+Business Media LLC, 2008, pp. 4.

[2] K. D. Timmerhaus and R. P. Reed, "Historical Summary of Cryogenic Activity Prior to 1950" in *Cryogenic Engineering*. 1st ed., vol. 2. R. Radebaugh, Ed Boulder, CO 80309: Springer Science+Business Media LLC, 2008, pp. 5.

[3] K. D. Timmerhaus and R. P. Reed, "Historical Summary of Cryogenic Activity Prior to 1950" in *Cryogenic Engineering.* 1st ed., vol. 2. R. Radebaugh, Ed Boulder, CO 80309: Springer Science+Business Media LLC, 2008, pp. 6-10.

[4] D. G. Henshaw, D. G. Hurst and N. K. Pope, "Structure of Liquid Nitrogen, Oxygen, and Argon by Neutron Diffraction." *American Physical Society,* vol. 92, pp. 1229-1234, Dec. 1953.

[5] N. Harish, "Advance Technology for Spices Grinding a Review." *International Journal of Agricultural Science and Research,* vol. 7, pp. 529-536, Jun. 2017.

[6] Yu. V. Gorbatskii, V. E. Gerasimov, V. A. Peredel'skii, R. V. Darbinyan, A. I. Lyapin and N. I. Izotov, "Use of LNG cryogenic technology during refining of associated petroleum gases." *Chemical and Petroleum Engineering*, vol 4 0 pp. 525-527, Sept. 2004.

[7] R. M. George, "Freezing processes used in the food industry." *Trends in Food Science & Technology*, vol 4, pp. 134-138, May. 1993.

[8] P. Jain, P. Agarwal, D. Mathur, P. Singh and A. Sharma, "Evolution of cryogenics - A review on applications of cryogenics in medicine." *Materials Today P roceedings,* vol 47, pp. 3059-3063, March 2021.

[9] L. C. Chow, W. F. Lu, O. J. Hahn, M. S. Sehmby, C. J. Chui and M. R. Pais, "Fundamental Studies in Cryogenic Cooling of Power Electronics (No. WL-TR-95-2116)." *Wright Interim,* vol 9, pp.12, Oct. 1995.

[10] A. R. Jha, *Cryogenic Technology and Applications*. Burligton, MA, 2006, pp. 1-60.

[11] Shujianyang, "YF-77 cryogenic rocket engine, displayed at China Science and Technology Museum." Internet: https://en.wikipedia.org/wiki/YF-77, June 23, 2023 [Dec. 12, 2023].

[12] “Cern Large Hadron Colinder.” Internet: https://home.cern/science/accelerators/large-hadron-collider [Nov. 12, 2023].

[13] A. David, “Cms Pins Down Higgs with First Run Data Cern.” Internet: https://home.cern/news/news/accelerators/cms-pins-down-higgs-first-run-data [Dec. 8, 2023].

[14] F. Marignetti and G. Rubino, “Perspectives on Electric Machines with Cryogenic Cooling.” *Energies*, vol 16, pp. 2994, Feb. 2023.

[15] E. Tsolakis, C. Kalligeros, P. Tzouganakis, D. Koulocheris and V. Spitas, “A novel experimental setup for the determination of the thermal expansion coefficient of concrete at cryogenic temperatures.” *Construction and Building Materials*, vol 30 9 pp. 1-16, Nov. 2021.

[16] A. A. Khan and M. I. Ahmed, “Improving tool life using cryogenic cooling.” *Journal of Materials Processing Technology*, vol 196, pp. 149-154, May. 2008.

[17] N. R. Dhar, S. Paul and A. B. Chattopadhyay “Machining of AISI 4140 steel under cryogenic cooling tool wear, surface roughness and dimensional deviation.” *Journal of Materials Processing Technology*, vol 123, pp. 483-489, May 2002.

[18] R. Xue, X. Lin, Y. Ruan, L. Chen and Y. Hou, “Cooling performance of multi-nozzle spray with liquid nitrogen.” *Cryogenics*, vol 121, pp. 1-5, Jan, 2022.

[19] R. B. Jacobs, “Cryogenic Liquid Consumption: Limits and Estimation,” in *Advances in Cryogenic Engineering* 1st ed., vol. 1 Timmerhaus, K.D Ed. Boston, MA: Springer Science, 1963, pp. 556-620.

[20] Z. Zong, “Specific liquid requirement to cool down cryogenic equipment.” *Cryogenics*, vol 119, pp 1-3, Oct. 2021.

[21] A. Hofmann, “The thermal conductivity of cryogenic insulation materials and its temperature dependence.” *Cryogenics*, vol 46 pp. 815-824. Nov. 2006.

[22] J. E. Fesmire, “Standardization in Cryogenic Insulation Systems Testing and Performance Data.” *Physics Procedia*, vol 67, pp.1089-1097, Oct. 2015.

[23] National Institute of Standards and Technology, “Low-Temperature Properties of Silver.” *Journal of Research of the National Institute of Standards and Technology*, vol 1, pp. 129, March 1995.

[24] R. B. Jacobs, “Cryogenic Liquid Consumption: Limits and Estimation,” in *Advances in Cryogenic Engineering* 1st ed., vol. 1 Timmerhaus, K.D Ed. Boston, MA: Springer Science, 1963, pp. 556-620.

[25] K. Wark, (1955, Nov.), “Tables of Thermal Properties of Gases.” *Nvlpubs* vol 1 pp. 564, Nov. 1955.

[26] Z. Zhang and M. B. Pate, “A Methodology for Implementing a Psychrometric Chart in a Computer Graphics System.” *Ashrae*, vol 94, Jan 1988.

[27] “Izocam Calculation Programs.” Internet: https://www.izocam.com.tr/tr/teknik-bilgiler/hesaplama-programlari [Oct. 15, 2023].

[28] Ashrae, “Table of Contents: 2018 Ashrae Handbook-Refrigeration.’’ Internet: https://www.ashrae.org/technical-resources/ashrae-handbook/table-of-contents-2018-ashrae-handbook-refrigeration, Dec. 13, 2018 [Sep. 25, 2023].

[29] J. E. Fesmire, “Layered Thermal Insulation Systems for Industrial and Commercial Applications. NASA Tech Briefs Web.” Internet: https://ntrs.nasa.gov/archive/nasa/casi.ntrs.nasa.gov/20150018118.pdf, Aug. 15, 2015.

[30] Izobir, “Cold Storage Insulation.” Internet: https://www.izobir.com/soguk-hava-depolari-izolasyonu [Sep. 25, 2023].

[31] J.J. Dunn and D.S. Bergstrom, “AL 2003tmldss (Uns S32003) as a substitute for type 316L. Revue de Métallurgie.” 104(7-8), pp.359–366. Internet: https://www.researchgate.net/publication/232022008_AL_2003_LDSS_UNS_S32003_as_a_substitute_for_type_316L, July, 2007 [Dec. 24, 2023].

[32] MatWeb, “Aisi Type 316L Stainless Steel, annealed sheet.” Internet: https://www.matweb.com/search/DataSheet.aspx?MatGUID=a2d0107bf958442e9f8db6dc9933fe31&ckck=1 [Dec. 5, 2023].

[33] Acme, “Acme Plastics What is Acrylic/Plexiglass Acme Plastics.” Internet: https://www.acmeplastics.com/what-is-acrylic-plexiglass [Dec. 5, 2023].

[34] MatWeb, “Overview of materials for Acrylic Data Sheet.” Internet: https://www.matweb.com/search/datasheet.aspx?bassnum=O1303 [Dec. 5, 2023].

[35] Gnee, “Steel S235JR Steel Plate.” Internet: https://www.gneesteel.com/products/steel-plate/index_20.html [Dec. 5, 2023].

[36] MatWeb, “Overview of material for S235JR EN10025-2 (ref) Steel, +AR.” Internet: https://www.matweb.com/search/DataSheet.aspx?MatGUID=96a3d2463ccb43e3a6c4a48eb0417f13 [Dec. 5, 2023].

[37] P. M. Knupp, “Remarks on Mesh Quality. Presentation at the 45th Aiaa Aerospace Sciences Meeting and Exhibit Sandia National Laboratories.” Internet: https://www.osti.gov/servlets/purl/1146104S0011227506001160, Jan. 15, 2007 [Dec. 8, 2023].

[38] Ansys Help, “Mesh Metrics Explainedfeatips.com.” Internet: https://featips.com /2022/11/21/ansys-mesh-metrics-explained, Feb. 15, 2023 [Dec. 5, 2023].

[39] M. Ozen and Fellow, “A. S. M. E. Meshing Workshop. In Meshing Workshop (Vol. 25).” Internet: www.ozenınch.com, Nov. 25, 2011 [Dec. 5, 2023].

[40] Ansys Help, “Mesh Metrics Explainedfeatips.com.” Internet: https://featips.com /2022/11/21/ansys-mesh-metrics-explained, Feb. 15, 2023 [Dec. 5, 2023].

[41] M. Ozen and Fellow, “A. S. M. E. Meshing Workshop. In Meshing Workshop (Vol. 25).” Internet: www.ozenınch.com, Nov. 25 2011 [Dec. 6, 2023].

[42] R. B. Jacobs, “Cryogenic Liquid Consumption: Limits and Estimation,” in *Advances in Cryogenic Engineering* 1st ed., vol. 1 Timmerhaus, K.D Ed. Boston, MA: Springer Science, 1963, pp. 556-620.

[43] “MGM Statistics.” Internet: https://www.mgm.gov.tr/veridegerlendirme/il-ve-ilceler-istatistik.aspx, Oct. 10, 2018 [Nov. 10, 2023].

[44] Auguste Cryogenics, “Auguste Cryogenics Main.” Internet: https://augustecryogenics.com, Jan. 10, 2021 [Nov. 12, 2023].

[45] Auguste Cryogenics, “Liquid Cylinders.” Internet: https://augustecryogenics.com/products/liquid-cylinders/, Jan. 10, 2021 [Oct. 10, 2023].